RECOMBINATION KINETICS IN CdS

by

DONALD WALTER NYBERG

B.A.Sc., University of British Columbia, 1957
M.A.Sc., University of British Columbia, 1960

A THESIS SUBMITTED IN PARTIAL FULFILLMENT OF

THE REQUIREMENTS FOR THE DEGREE OF

DOCTOR OF PHILOSOPHY

in the Department

of

Physics

SIMON FRASER UNIVERSITY

November, 1967

EXAMINING COMMITTEE APPROVAL

_____ K. Colbow
Senior Supervisor

_____ R. F. Frindt
Examining Committee

_____ J. C. Irwin
Examining Committee

PARTIAL COPYRIGHT LICENSE

I hereby grant to Simon Fraser University the right to lend my thesis or dissertation (the title of which is shown below) to users of the Simon Fraser University Library, and to make partial or single copies only for such users or in response to a request from the library of any other university, or other educational institution, on its own behalf or for one of its users. I further agree that permission for multiple copying of this thesis for scholarly purposes may be granted by me or the Dean of Graduate Studies. It is understood that copying or publication of this thesis for financial gain shall not be allowed without my written permission.

Title of Thesis/Dissertation:

_____

_____

_____

_____

Author: _____

(signature)

_____

(name)

_____

(date)

ABSTRACT

In high-purity cadmium sulfide crystals, at low temperatures and high excitation intensities, emission lines attributed to free and bound exciton recombination are observed in the spectral range 4860 to 5090 Å. In addition, the main peaks of two broad emission bands, which are repeated at lower energies with the simultaneous emission of one or more longitudinal optical phonons, are observed at about 5140 and 5180 Å. The high energy band, which is dominant at liquid nitrogen temperatures, is due to free electrons recombining with holes bound at cadmium vacancy acceptors. The low energy band, which is dominant at liquid helium temperatures, is due to electrons bound to shallow donors recombining with the bound holes.

The photoluminescence efficiency and photoconductivity response of cadmium sulfide crystals were measured and the data interpreted in terms of an energy band model involving the donor and acceptor levels previously established as being involved in the radiative transitions. In addition, an effective recombination center (consisting of deep acceptor-like recombination centers) and non-radiative surface recombination centers are required to account for the non-radiative transitions. The results of the thesis are divided into four topics and are summarized below.

The first topic deals with the controversy in the literature regarding the origin of the high energy emission band at about 5140 Å. Two recent papers, which identify this band as being due to bound electron-to-bound hole transitions, are analyzed and it is shown that their conclusions are incorrect. Further

analysis and experiments show that their data support the free electron-to-bound electron interpretation of other authors.

The second topic was the effect of surface recombination centers on the luminescence efficiency. These states are believed to be mainly chemisorbed oxygen ions. Non-radiative surface recombination is reduced by applying an electric field to counteract the electric field in the charge depletion layer next to the surface, or by photo-desorbing the oxygen ions. This electric field draws minority carriers to the surface where they recombine non-radiatively. The luminescence efficiency is found to be lowest when the electron-hole pairs are generated, closest to the surface. This is interpreted as meaning that a greater fraction of the carriers can reach the surface to recombine and that ambipolar diffusion of carriers into the interior of the crystal does not take place. It was also found that heating CdS briefly in a nitrogen ambient produces free-to-bound and bound-to-bound transitions associated with nitrogen acceptors 130 meV above the valence band. The nitrogen impurities are near the surface since these bands are removed by a short etch in concentrated hydrochloric acid.

The third topic was the recombination kinetics of excitons and the bound electron-to-bound hole luminescence. In all cases, the exciton efficiency increases with increasing excitation intensity as expected since the formation of excitons depends on the product of the free carrier densities. The bound-to-bound emission efficiency is high and varies slowly with excitation intensity. The efficiency falls slowly both at high and at

low excitation intensity. The fall-off in efficiency at high excitation intensity is accompanied by an increase in efficiency of the free-to-bound emission band. The decrease in efficiency at low excitation intensities may be due to non-radiative surface recombination.

The last topic was the recombination kinetics of the free electron-to-bound hole luminescence. Using the energy band model mentioned earlier, the data was analyzed to obtain the electron and hole lifetimes, the luminescence efficiency, and the electron and hole capture cross-sections of the cadmium vacancy acceptor and the other deep recombination center. The internal luminescence efficiency is near unity as long as the minority carriers (holes) are quickly captured by the radiative recombination centers (cadmium vacancies). At high temperature the luminescence efficiency is low because the cadmium vacancy centers act as traps rather than recombination centers, while at high excitation intensities the efficiency drops because the radiative transitions saturate.

TABLE OF CONTENTS

LIST OF FIGURES

ACKNOWLEDGMENTS

I wish to thank Dr. K. Colbow for his guidance throughout the course of this work, and for his advice and constructive criticism during the preparation of this thesis. I also wish to thank the many other members of the Physics Department with whom I have had valuable discussions.

The assistance of the National Research Council of Canada and the Defense Research Board of Canada in providing research facilities for this work is also gratefully acknowledged.

CHAPTER I

INTRODUCTION

This thesis describes an experimental investigation and a detailed analysis of the recombination kinetics in cadmium sulfide crystals. The experiments entailed measuring the photoluminescence and the photoconductance as functions of the excitation intensity and wavelength at various temperatures. The effects of crystal resistivity, surface condition, and of an applied electric field on the luminescence and photoconductance were also evaluated. With a simple, but realistic, energy band model, and a detailed theoretical analysis, it was possible to deduce the fundamental parameters governing the recombination kinetics.

Before proceeding with the central theme of the thesis, it is valuable to review the present knowledge of luminescent processes in cadmium sulfide. The remainder of the introduction is devoted to this task.

The luminescence spectrum of cadmium sulfide has been extensively studied. At low temperatures and high excitation intensities, narrow emission lines attributed to free and bound exciton recombination are observed in the spectral range 4860 to 5090 Å (Thomas and Hopfield, 1961, 1962; Reynolds and Litton, 1963). Information on these lines has been summarized in a review article by Reynolds (1965). At liquid helium temperatures the two main exciton emission lines are I_1 and I_2. Line I_1 occurs when an exciton bound to a neutral acceptor decays and line I_2 when an exciton bound to a neutral donor decays.

Frequently, at high resolution, I_2 is seen to consist of several lines, corresponding to excitons bound at different types of donors. These excitons are only weakly bound to these centers and hence are not seen at higher temperatures. Above 60°K, the main exciton emission line is the free exciton, "A". The temperature dependence of these excitons have been investigated by Bleil and Albers (1964). These exciton emission lines are only slightly phonon broadened because both the free and the bound excitons are only weakly coupled to the lattice.

In addition to the exciton lines, two broad green emission bands have been observed (Kröger, 1940; Klick, 1951; Furlong, 1954; Furlong and Ravilious, 1955; Bancie-Grillot et al., 1959; Pedrotti and Reynolds, 1960) between 5100 and 5200 Å. Phonon replicas of these bands are repeated at lower energies through the simultaneous emission of one or more longitudinal optical phonons. As a result of the work of these investigators, the spectral position and shift with temperature of these bands was well established. Typical spectra of this green edge luminescence seen under D.C. photoexcitation are shown in Fig. 1. At 2°K, two no-phonon emission bands are seen: a high energy band peaked at 5140 Å and a low energy band at 5180 Å. Both bands are repeated with decreasing amplitude at intervals of the longitudinal optical phonon energy (38 meV). The relative strength of the two bands varies with excitation intensity and from crystal to crystal, although the low energy band is usually dominant. At 78°K, the low energy band is normally missing and only the high energy band is observed.

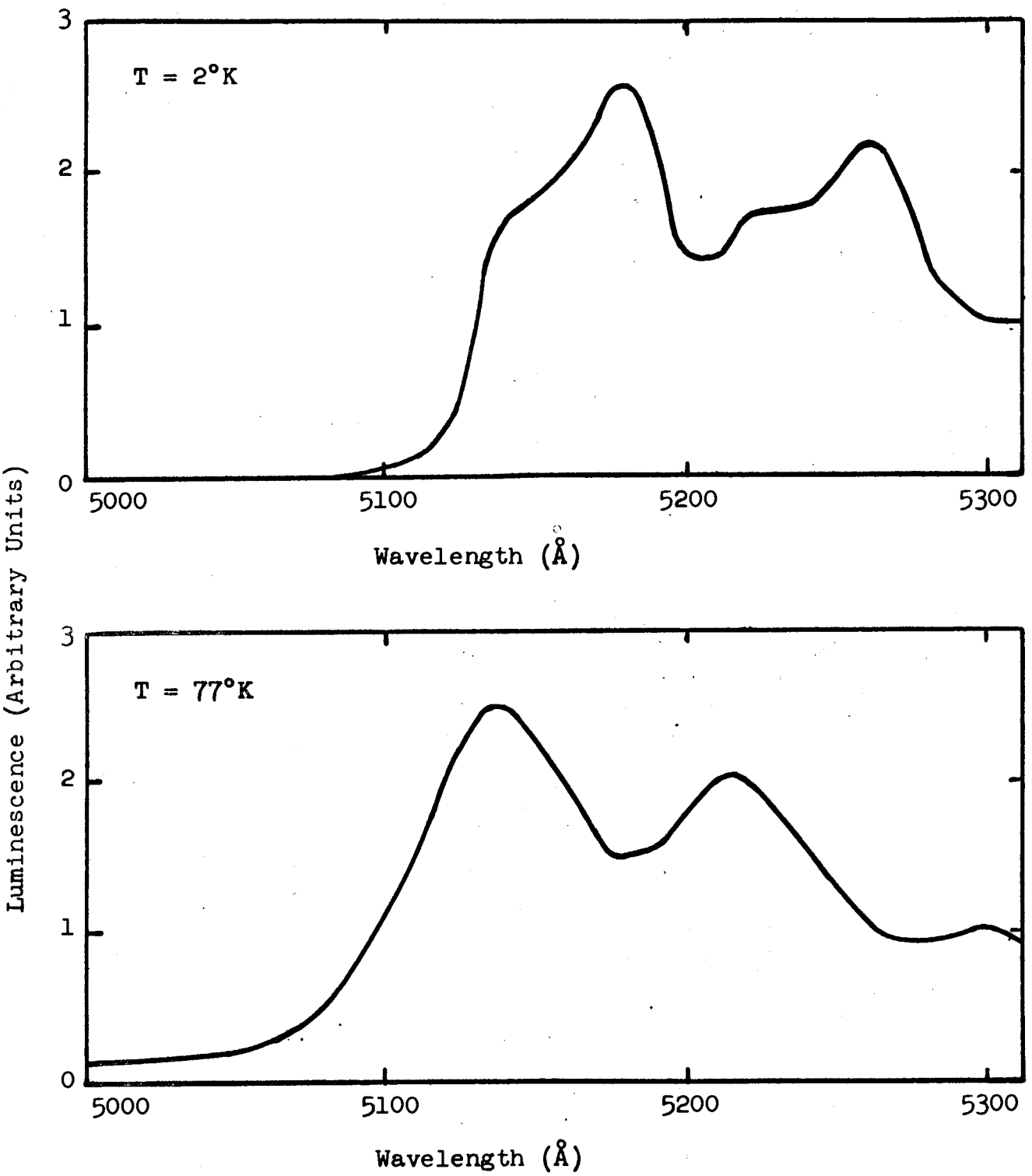

FIG. 1: GREEN EMISSION FROM A TYPICAL LUMINESCENT CdS CRYSTAL

The origin of these bands has been the subject of considerable controversy which has now been resolved, in part as a result of the work reported in this thesis. To Kroger and Meyer (1954), the large coupling of these radiative transitions with the longitudinal optical phonons suggested recombination of free holes and free electrons through exciton states as their origin. However, Hopfield (1959) showed theoretically that the phonon replicas of these bands could only be understood by a mechanism involving trapped carriers. The basic reason is that, when recombination takes place in the field of an impurity, the impurity can absorb crystal momentum. Lambe et al (1956) proposed a free hole-to-trapped electron recombination model at $4^{o}K$, while Collins (1959) showed that, after excitation, the free holes decay much faster than the green emission at $77^{o}K$ and proposed a free electron-to-bound hole recombination model.

Thomas and Hopfield (1959) suggested two alternative models. The first explanation assumes the green emission to be the result of the recombination of electrons in minima not at k=0 with trapped holes. The shift toward longer wavelengths would occur by assuming that the off-axis minima move toward k = 0 as the temperature decreases. Their second explanation assumes that a bound state of an electron exists in the vicinity of a trapped hole. At high temperatures (e.g. $77^{o}K$), the recombination would take place from the unbound states, e.g. from the conduction band to a trapped hole, while at low temperature (e.g. $4.2^{o}K$) the recombination would take place from the bound state of the electron to the bound state of the hole. The energy difference

between the bound and unbound states of the electron would account for the shift in wavelength of the peak of the emission band. Pedrotti and Reynolds (1960) postulated a free electron-to-bound hole transition at 77°K and a bound electron-to-bound hole transition at 4°K, in agreement with Thomas and Hopfield's second model. Their data also showed that as the crystal was cooled one peak disappeared and the other appeared. If the first model suggested by Thomas and Hopfield were correct, a gradual shift of the peak would occur. The fact that free electrons rather than free holes are involved in the luminescence at 77°K was further supported by Spear and Bradbury (1965) by photoconductivity and luminescence measurements.

Conflicting views were proposed by Halsted and Segall (1963) who suggested a bound-exciton recombination at a double acceptor level near the conduction band, and Razbirin (1964) who proposed that the emission results from the annihilation of an exciton with simultaneous ionization of a trapped hole. Gross, Razbirin and Permogorov (1965) proposed that both transitions were of the bound-to-bound type, originating from different shallow donors and terminating on the same acceptor. However, since the higher energy emission is dominant at higher temperatures, Gross's model would imply that the more tightly bound donor electrons are thermally ionized first. This model was also reported by Gross and Nedzvetsky (1965).

Colbow (1966) observed time-resolved photoluminescence spectra of the green bands as a function of temperature. From the wavelength shift of the emitted light with time and temperature, he

concluded that the high energy band (5140 Å) was due to the recombination of free electrons with holes bound at acceptors 170 meV above the valence band, while the low energy band (5180 Å) was due to the recombination of electrons bound at donors 30 meV below the conduction band with the bound holes. In addition to values for the donor and acceptor binding energies, the bound-to-bound reaction coefficient and an estimate of the donor concentration were obtained. The conclusions were supported by independent information from the time decay of the bound-to-bound and the free-to-bound emission intensity, and its correlation with the low temperature decay of photoconductivity as a function of time after excitation. The strong coupling of the trapped carriers with the lattice is in part responsible for the broadness of the free-to-bound and the bound-to-bound emission bands. Colbow (1966) found shoulders on these bands which were attributed to the simultaneous emission or absorption of transverse optical (TO_2) and acoustical phonons .

In recent work, Maeda (1965) and Condas and Yee (1966), again proposed a bound electron-to-bound hole transition for the high energy band. Maeda (1965) based his conclusions on the different activation energies for thermal quenching of the green luminescence in conducting and insulating crystals. However, if correctly interpreted (Chapter III), his data confirms that the high energy band is due to a free electron-to-bound hole transition. Condas and Yee observed a small shift of the peak of the high energy band with excitation intensity. They based their conclusions on the nature of the transition on the assumption that such a shift

could only be observed in a bound-to-bound transition. However, in Chapter III, it has been shown that the small shifts observed can reasonably be explained for a free-to-bound transition by either a reduced acceptor binding energy due to free carrier screening or by a photoexcited electron temperature larger than the lattice temperature.

Thus, to summarize the work on the green emission bands, it is now well established (in part as a result of the work reported in this thesis) that the low energy band at 5180 Å is due to electrons, bound at donors 30 meV below the conduction band, recombining with holes, bound at acceptors 170 meV above the valence band. The high energy band at 5140 Å is due to free electrons recombining with the bound holes.

The shallow donors are believed to be group III and VII impurities such as aluminum and chlorine, while the deep acceptors are most likely caused by cadmium vacancies and the group I impurities copper and silver (Woodbury, 1964). Handelman and Thomas (1965) have shown that the conductivity of high-purity CdS crystals can be reproducibly changed between conducting (resistivity less than 10 ohm-cm) and insulating (resistivity greater than 10^8 ohm-cm) by heat treatment in cadmium vapor and vacuum respectively. The heat treatment changes the density of cadmium vacancies and thus the degree of compensation of the donors. In addition, both free-to-bound and bound-to-bound recombination associated with a new acceptor level 130 meV above the valence band due to nitrogen impurities have been observed (Chapter IV).

As stated earlier, the primary aim of this work was to investigate the recombination kinetics in photoluminescent cadmium sulfide crystals. One might expect for a wide-band-gap semiconductor, containing fairly shallow impurity states, that non-radiative recombination is an uncommon process since it would require the emission of many phonons simultaneously. Some non-radiative bulk recombination may, however, be expected through the presence of non-radiative centers due to crystal defects and impurity clusters. On the other hand, the surface may be expected to give rise to mainly non-radiative recombination, since there may be a large density of recombination centers in the forbidden band gap. These states may be either intrinsic or extrinsic. In 1932, Tamm predicted theoretically the existence of localized states associated with the termination of the periodic crystal potential. Surface states associated with foreign impurities have been extensively investigated in silicon and germanium. Recently, Levine and Mark (1966), have predicted and apparently observed intrinsic surface states on ionic crystals using photoconductivity techniques. However, most of the non-radiative surface recombination is believed to occur at extrinsic surface states arising from adsorbed impurities such as oxygen which strongly affect the surface recombination (Bleil and Albers, 1964). Thus, for strongly absorbed light, it is expected that the surface will have a dominant role in determining the luminescence efficiency, while for weakly absorbed light, bulk non-radiative recombination should be the more important.

DeVore (1956) has made a theoretical analysis of the shape of the

photoconductivity spectral distribution curves. The analysis is based on the effects of surface and volume recombination on the optically generated free electrons as the excitation wavelength and hence the absorption coefficient is varied. Mark (1965a) has extended this analysis to the case of an insulator with two carriers. In Appendix A, the analysis of DeVore and Mark has been extended to include the effects of an applied electric field.

The thesis is organized into seven chapters. Following this introduction there is a chapter on experimental techniques which describes the apparatus and procedures used in obtaining the data. The third chapter deals with the controversy in the literature regarding the origin of the high energy green emission band at 5140 Å. The next three chapters deal with the major experimental results of this study: surface effects on photoluminescence; bound-to-bound and exciton recombination kinetics; and, free-to-bound recombination kinetics. The last chapter contains a summary of the work and the major conclusions along with suggestions about possible future research.

CHAPTER II

EXPERIMENTAL TECHNIQUES

1. Apparatus

The experimental arrangement used to study photoluminescence is illustrated schematically in Fig. 2. The samples were mounted in holders (Fig. 3), and immersed in liquid helium, nitrogen or oxygen coolant on the end of a long stainless steel rod. The crystals were excited by the light from a PEK Labs (model 911) 100 watt high pressure mercury arc which was dispersed by a Jarrell-Ash (model 82-410) 0.25 meter Ebert monochromator with a grating of 1180 grooves per millimeter blazed at 3000 Å. Two millimeter wide slits were used and this restricted the excitation wavelengths to a band about 100 Å wide. The emission spectrum of the light source consists of intense pressure broadened bands at the mercury emission lines superimposed on a broad continuous background. At each excitation wavelength the spectrum of the excitation light was measured and Corning Glass Color Filters chosen so as to eliminate any unwanted light from the intense bands in other regions of the spectrum. At all times, a Corning 7-59 filter was used at the exit slit of the monochromator to remove green and blue light of the same wavelengths as the luminescence. With this arrangement it was possible to achieve maximum excitation intensities of about 10 milliwatts per cm^2 at the crystal surface. The method of measuring the excitation intensity is described in the next section. The excitation intensity was controlled with Kodak Wratten neutral density filters.

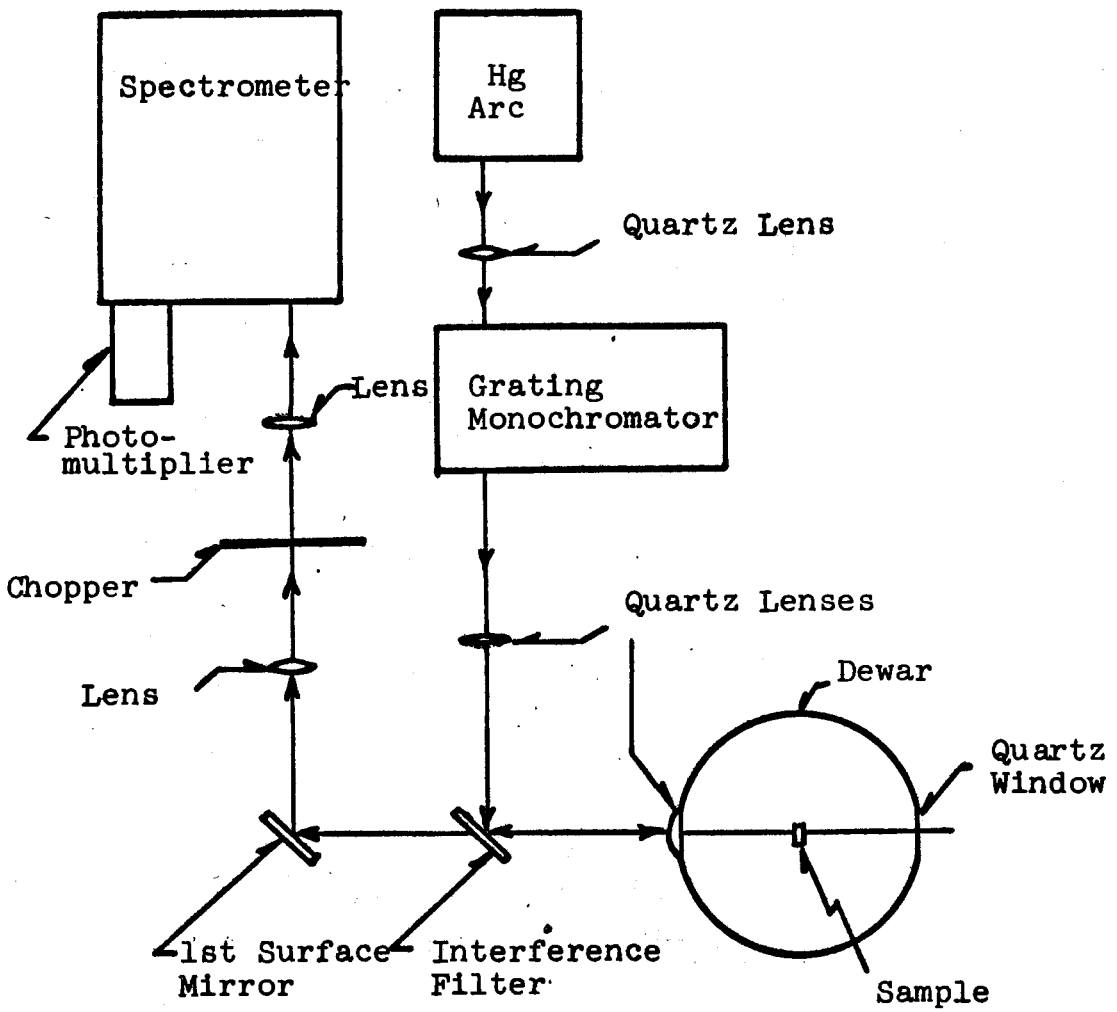

Fig. 2: Experimental Arrangement for Photoluminescence Measurements.

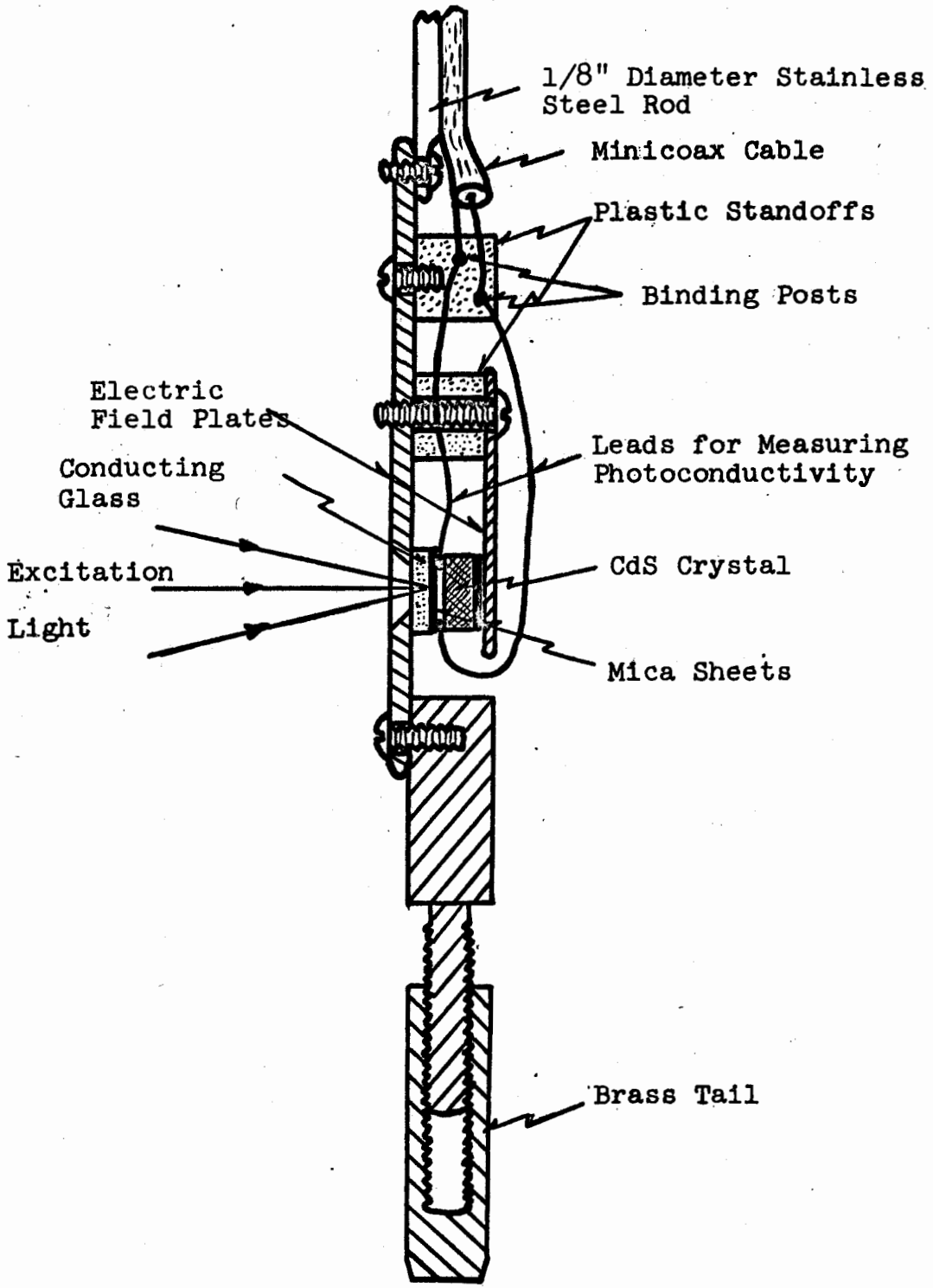

Fig. 3a: Sample Holder.

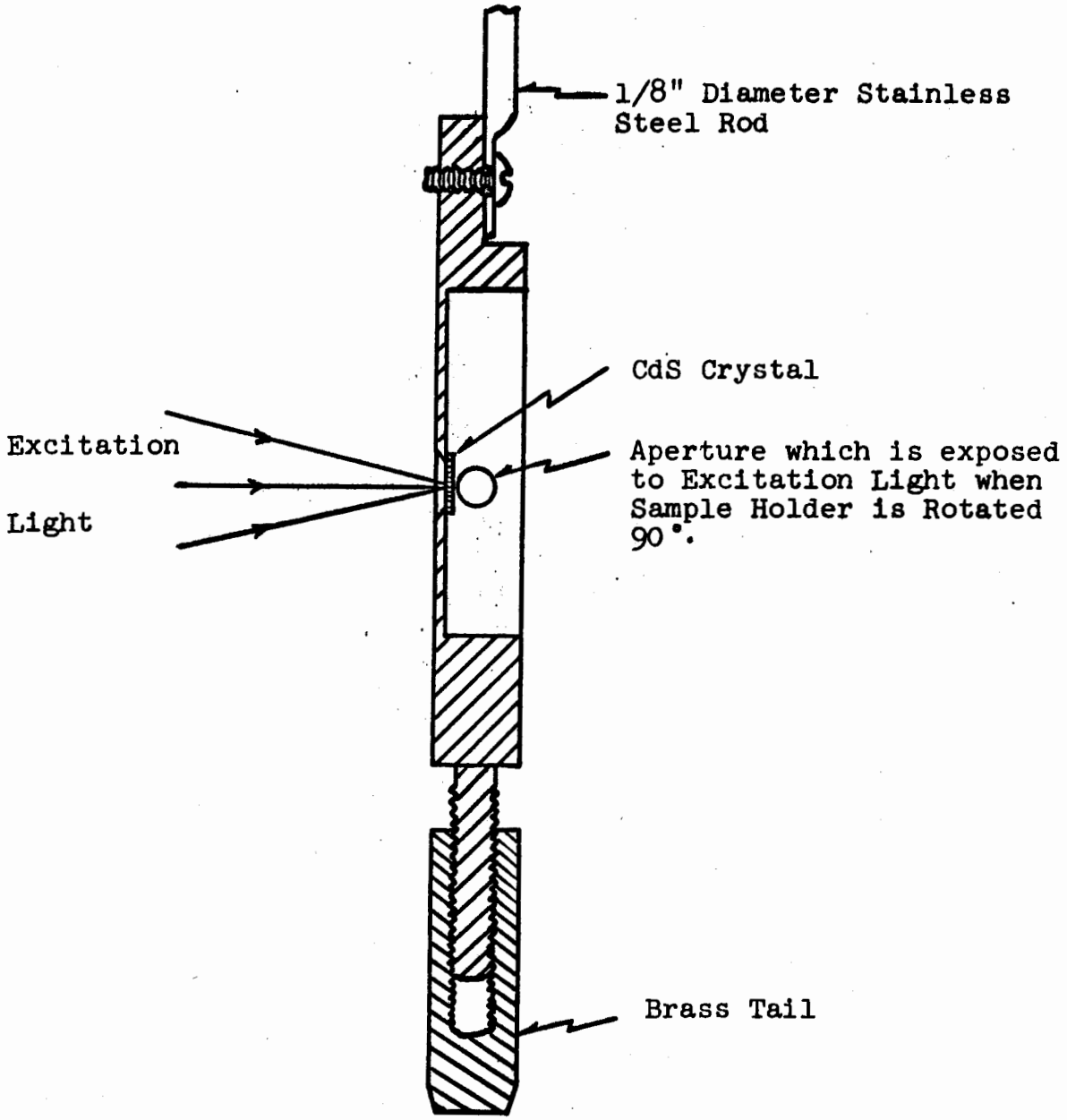

Fig. 3b: Sample Holder.

Part of the optical system was common to the excitation and detection systems. The excitation light was reflected off an interference filter (Optics Technology Inc. Series 6085, Type 500W) which reflected wavelengths shorter than 4500 Å when placed at an angle of 45° to the incident light. The excitation light was then focussed onto the crystal by an f/2 quartz lens mounted on the glass dewar. This same lens collected the luminescence emitted by the crystal. The luminescence was transmitted by the interference filter, mechanically chopped, and the spectrum analyzed in second order by a Spex Industries (model 1700-II) Czerny-Turner monochromator with a Bausch and Lomb 1200 grooves per millimeter grating blazed at 1.3 microns. The light was detected at the exit slit with a EMI (type 9558) photomultiplier (S-20 response), displayed by a Princeton Applied Research (model HR-8) phase sensitive detector, and recorded on a Moseley (model 2D-2A) X-Y recorder. The wavelength response of the spectrometer was calibrated by means of the sharp emission lines of a low pressure mercury arc while the energy response was determined using a standard lamp (Electro Optics Associates, Type L-101).

In the photoconductivity experiments, ohmic contacts were made by soldering gold wires to the front surface of the crystal with indium (Smith, 1955). The area between the electrodes was then illuminated, and the change in resistance measured with a Keithley (model 600A) electrometer.

The crystals were mounted in the brass sample holders with rubber cement, the cement being applied along only one edge of

the crystal so that no strains were introduced upon cooling. Care was taken not to expose the cement to the excitation light, since the cement is photoluminescent in the green region of the spectrum.

2. Measurement of Photoluminescence Efficiency as a Function of Excitation Wavelength

In the measurement of photoluminesence efficiency as a function of excitation wavelength it was necessary to know the photon flux incident on the crystal at each band (100 Å wide) of wavelengths used and this required many precautions. To minimize changes in excitation beam cross-section and position on the crystal as the excitation wavelength was varied, the optical axis of the excitation system was aligned by means of a laser beam and the excitation beam was defocussed so that its image on the specimen holder was about ten times the area of the crystal. The power supply for the mercury arc was run off a constant voltage transformer to minimize line voltage fluctuations, and the lamp was allowed to warm up for at least one-half hour before data were taken.

The crystals were mounted behind an aperture in the sample holder (Fig. 3b) so that the area of excitation was controlled. The sample holder itself was accurately centered on the optical axis by a threaded tail which was tapped into a brass block which in turn was keyed to the bottom of the liquid helium chamber as shown in Fig. 4. Above the sample holder a brass "spider" centered the stainless steel rod. Rotating the sample

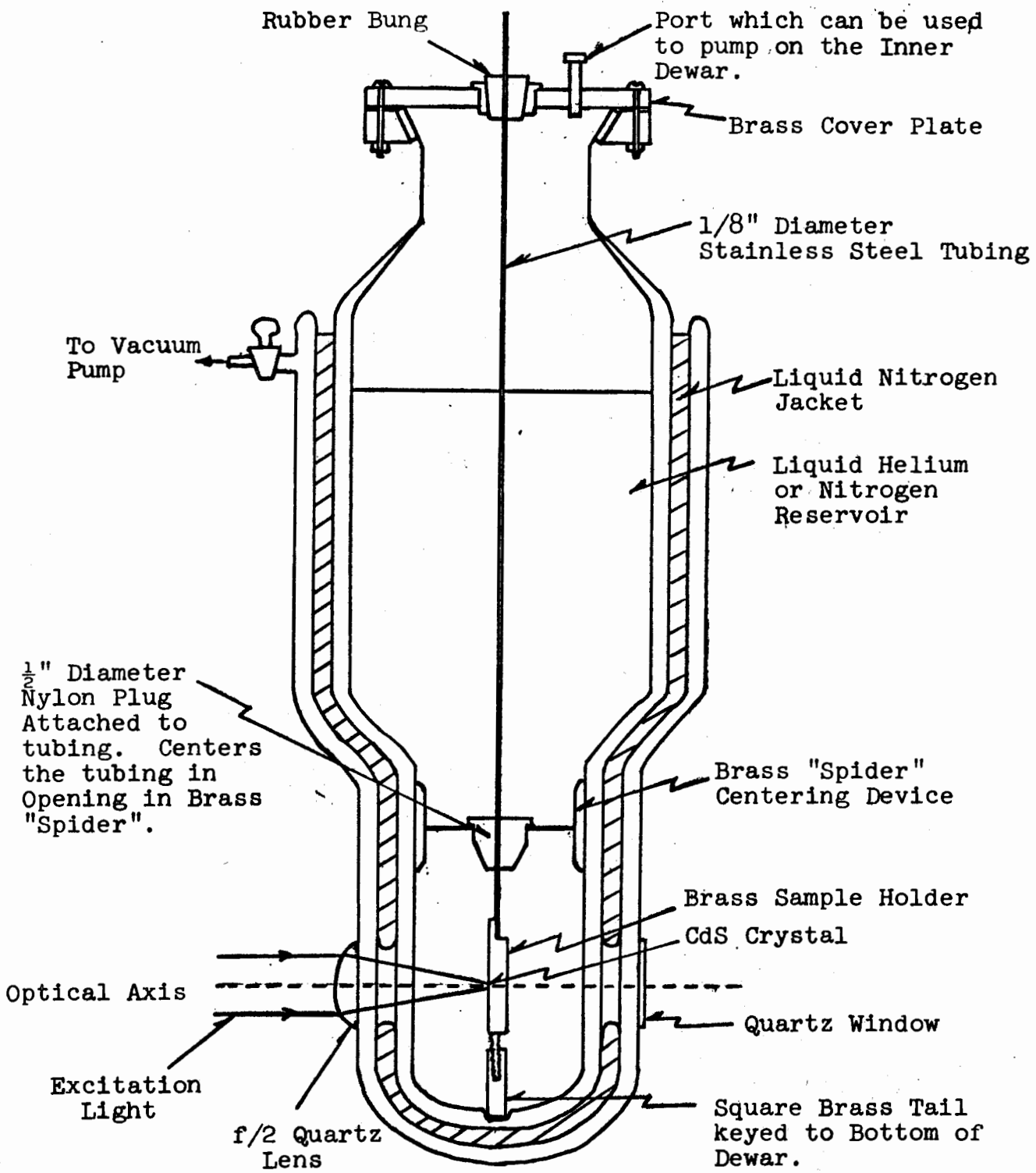

Fig. 4: Cross-Section of Liquid Helium Dewar showing Sample Centering Devices.

holder 90° exposed a second aperture at the position where the sample had been. Light passing through this aperture was collected at the rear of the dewar by a quartz lens and detected with an RCA 935 vacuum photodiode (S-5 response). In this way it was possible to calibrate the excitation lines immediately after performing the measurements of photoluminescence. The photon fluxes at each wavelength were arranged to be within a factor of two of the desired value by means of combinations of neutral density filters. The attenuation of the neutral density filters is a function of wavelength and they were calibrated with the RCA vacuum photo-diode by simply recording the signal before and after the filter was placed in the path of the excitation beam. Corning Glass Color Filters were used to attenuate unwanted intense lines in other regions of the spectrum as described in Section 1.

3. Electric Field and Oxygen Photodesorption Experiments

Photodesorption of oxygen from the crystal surface was performed by flushing the dewar with nitrogen gas while illuminating the crystal with strongly absorbed light. The photo-excited holes drift to the surface under the action of the strong electric field in the depletion layer near the surface. As the holes reach the surface, they neutralize the chemi-sorbed oxygen ions allowing them to leave the surface as the strong chemical bond is broken (Williams, 1962). Liquid nitrogen or helium coolant was then added without allowing oxygen gas to reach the crystal surface. This treatment also seemed to improve the reproducibility

of the measurements of luminescence efficiency as a function of excitation wavelength.

The electric field measurements were performed by placing the sample between sheets of mica and illuminating one face of the crystal through a transparent conducting glass electrode (Fig. 3a). Since neither electrode touched the sample, there was no possibility of electrical injection of carriers. Voltages of up to 4 KV were applied across the electrodes, which were about 1 mm apart. At 4.2°K, the applied voltage was limited to 1 KV by the lower breakdown voltage of helium gas.

4. Variable Temperature Measurements

Data at 4.2 and 2°K were taken using liquid helium and pumped liquid helium as the coolant. Pumped liquid helium was preferred because of the absence of bubbling in the superfluid phase. Temperatures between 64 and 77°K were achieved by pumping on liquid nitrogen and the temperature was obtained from the equilibrium vapor pressure in the dewar as registered by a mercury manometer. All data at temperatures below 78°K were taken using the dewar illustrated in Fig. 4.

In the temperature region between 80 and 100°K, where thermal quenching of the luminescence takes place, the variable temperature dewar illustrated in Fig. 5 was employed. The main advantage of this apparatus was that the temperature dependence of the photoluminescence was measured by cooling the crystals by gas flow rather than by immersion in liquid coolants. This avoids possible complications due to the different refractive

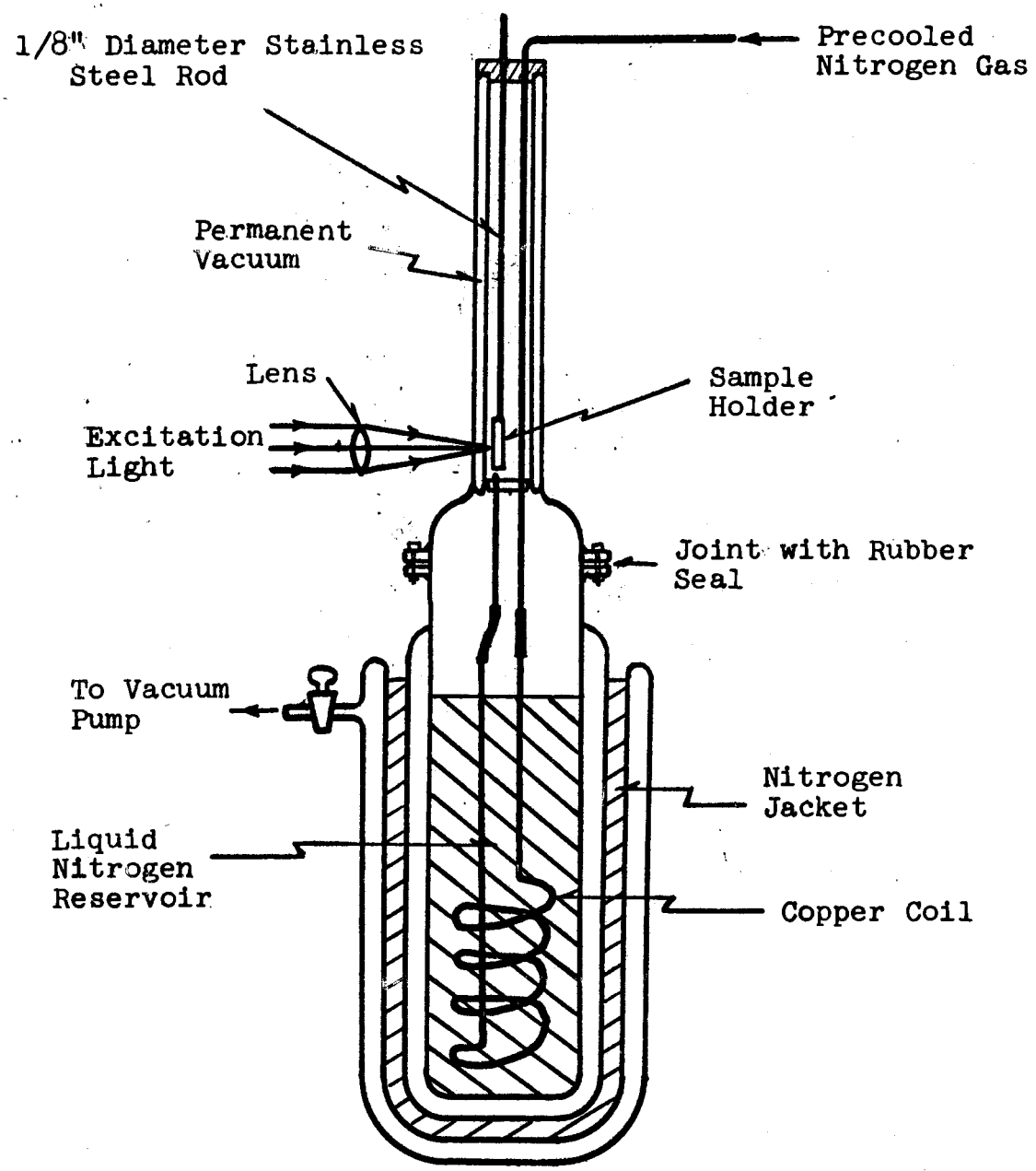

Fig. 5: Cross-Section of Variable Temperature Dewar.

indices of nitrogen and helium.

The principle of operation of the variable temperature dewar is as follows. Nitrogen gas from a storage cylinder flowed through a precooler coil immersed in liquid nitrogen, then down a stainless steel rod into a heat exchanger immersed in a large reservoir of liquid nitrogen in the bottom of the dewar. On leaving the heat exchanger, the gas was piped up to the neck of the dewar and vented just below the sample holder where the narrow constriction caused it to flow past the sample and on out the top of the dewar. Variable temperature was achieved by regulating the gas flow rate. Temperature measurement was by a gold-chromel thermocouple with the reference junction at liquid nitrogen temperature. Short term temperature stability of $\pm$ 1^{o}K was achieved. In this short time period (of the order of 5 minutes) it was possible to obtain a set of photoluminescence and photoconductance measurements over the useable range of excitation intensity.

5. Time Resolved Spectroscopy

In the experiments on the nitrogen acceptors described in Chapter IV, it was necessary to clearly identify the observed emission bands as free-to-bound and bound-to-bound. This is readily done using time resolution spectroscopy (Colbow, 1966) and the experimental arrangement is illustrated in Figs. 6 and 7

The sample was mounted in the dewar (Fig. 4) and excited about 10 times per sec by a brief (< 50 μ sec) flash of band-gap radiation (3000 - 4500 Å) from an EGG (type XFX 6B) xenon flash

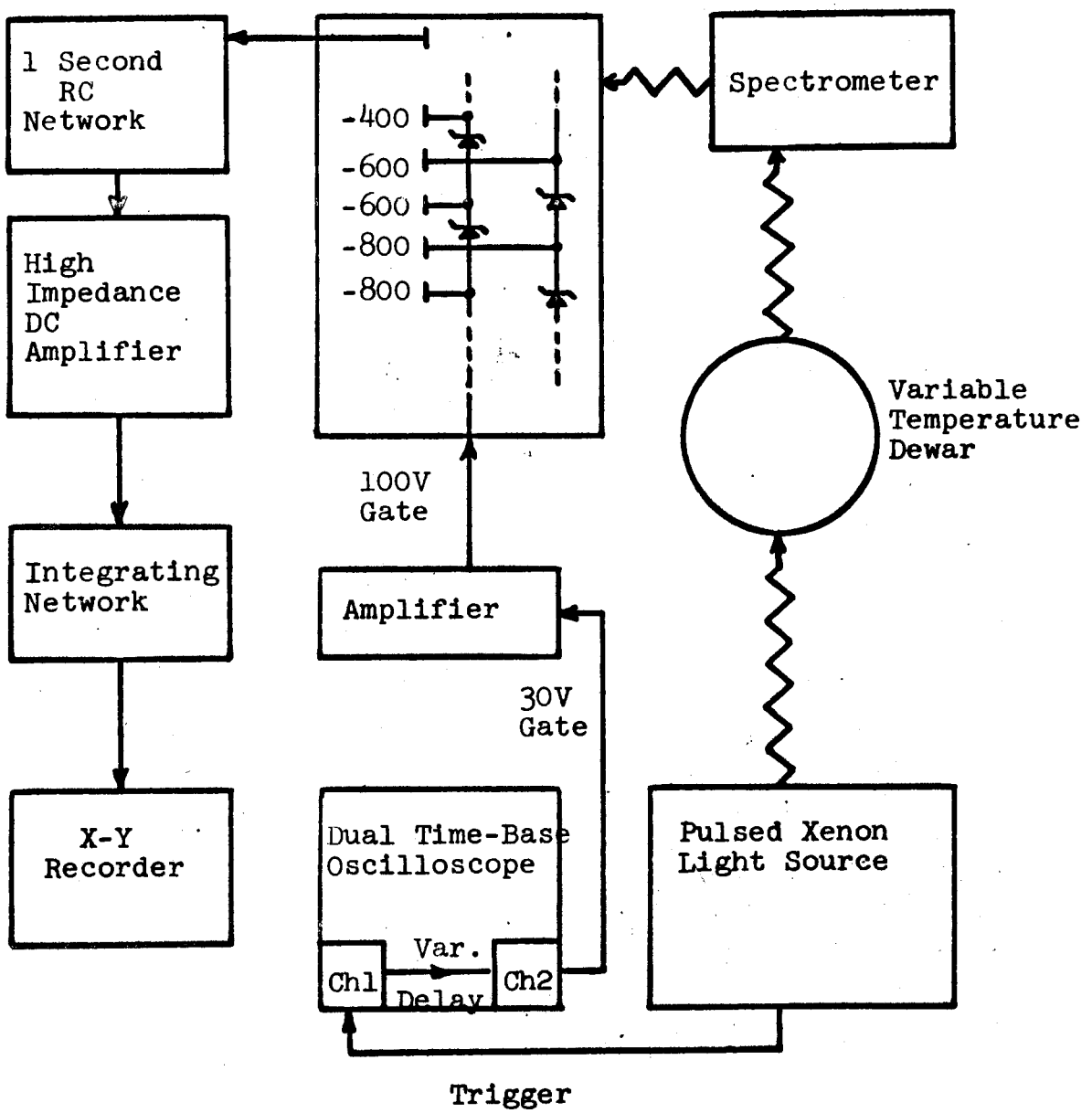

Fig. 6: Schematic of Time-Resolved Spectroscopy Set-up.

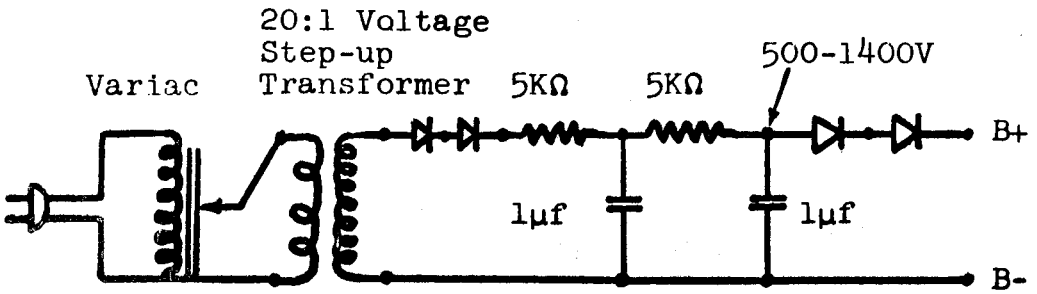

Power Supply

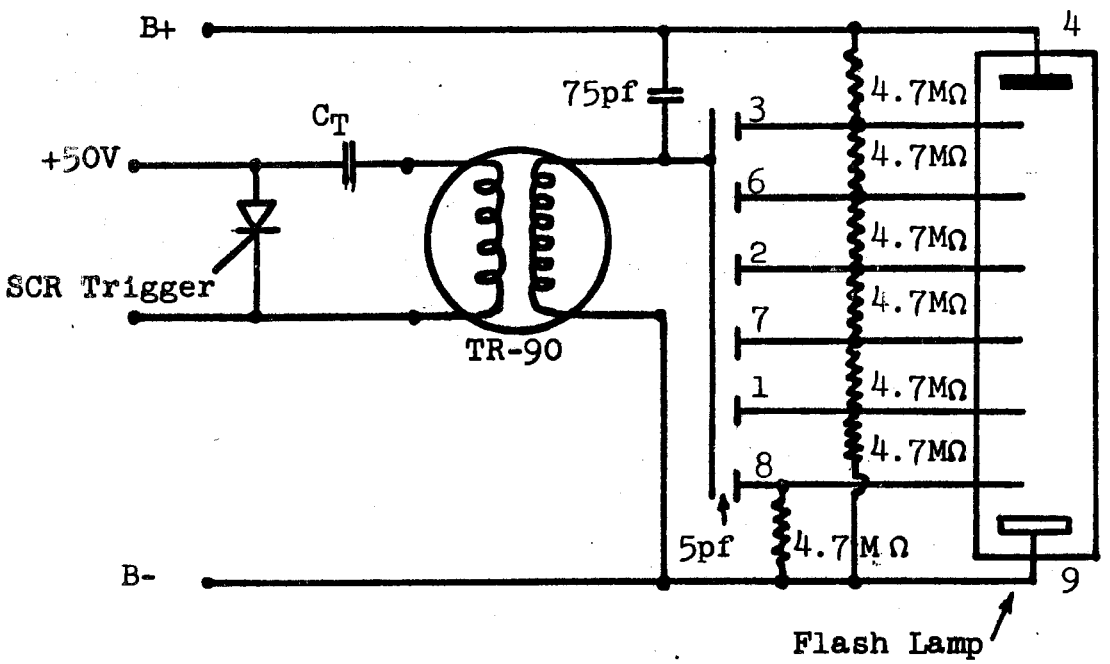

Trigger Circuit

FIG. 7: POWER SUPPLY AND TRIGGER CIRCUIT FOR XENON FLASH LAMP

tube. The luminescence from the crystal passed through the Spex Industries monochromator and was detected by a gated photomultiplier for a variable short time interval following a variable time delay after the excitation pulse. The resulting photomultiplier current pulses were fed through a 1-sec RC network, a high impedance D.C. amplifier (HP model 425A DC Microvoltmeter), and a 10-sec RC integrating network to a Moseley (model 2D-2A) X-Y recorder. With a slowly scanning monochromator the luminescence spectrum was recorded as a function of wavelength for the time interval after excitation when the photomultiplier is gated on.

The photomultiplier (EMI type 9558, S-20 photocathode) was operated in the following fashion (Colbow, 1966). In the absence of an excitation flash, two isolated strings of zener diodes and a D.C. supply of -2000V maintain neighboring pairs of successive dynodes at the same potential which differs by 200V from that of the following and the preceding pair. For this potential distribution, the current gain of the photomultiplier is very low. With each excitation flash an inductively coupled pulse triggers time base A of a Tektronix (model 555) dual-beam oscilloscope. Using the adjustable sweep time of time base B, and the variable time delay, an external positive gate of 30V (of variable duration and starting at a variable time after the triggering pulse) can be obtained. This gate is amplified to 100V and fed into one string of zener diodes, thus creating the usual conducting potential distribution, where successive dynodes are at a potential 100V above the previous

one. Hence the photomultiplier will detect light only while the gate is on.

CHAPTER III

FREE-TO-BOUND VERSUS BOUND-TO-BOUND RECOMBINATION CONTROVERSY

1. Introduction

As discussed in the introduction, the origin of the green emission bands whose no-phonon peaks occur at about 5140 and 5180 Å has been the subject of a great deal of controversy. Colbow (1966) showed that, after flash excitation, the time and temperature dependence of the afterglow can be understood by assuming that the high energy band at 5140 Å is due to a free electron-to-bound hole recombination, while the low energy band results from a bound electron-to-bound hole recombination. This work was in agreement with earlier work by Collins (1959) who postulated that the high energy band was due to a free electron-to-bound hole recombination, and by Pedrotti and Reynolds (1960) who postulated a free electron-to-bound hole recombination at 77°K and a bound electron-to-bound hole transition at 4°K. Conflicting views had been proposed by several earlier authors, as mentioned in the introduction, and these were discussed by Colbow (1966).

The evidence presented by Colbow (1966) that the high energy band was due to a free-to-bound transition seemed quite conclusive. However, about the same time, Maeda (1965) published his conclusions that the transition was of the bound-to-bound type. We will show that he had interpreted his data incorrectly, although this was not known at the time. More recently, Condas and Yee (1966), being aware of Maeda's work but not of the other

major papers on the subject, also postulated a bound-to-bound transition for this band. Since the interpretation of the recombination kinetics of this band (Chapter VI) is dependent on its origin, it is important to resolve these conflicting views. In the following two sections, these papers are analyzed and their results shown to be not in conflict with the free-to-bound recombination model.

2. Thermal Quenching of the Luminescence

The quenching of the green edge luminescence occurs at the temperature at which the bound holes become thermally ionized (Maeda, 1965 and Ch. VI). On the basis of the activation energies for the quenching mechanism, Maeda concluded that the high energy band is of the bound-to-bound type in disagreement with other work (Collins, 1959; Pedrotti and Reynolds, 1960; Colbow, 1966). However, if correctly interpreted, his data confirms that the high energy band is due to a free-to-bound transition, as shown by the following analysis.

The thermal ionization rate of holes bound at the cadmium vacancy acceptors is

$$\gamma = \sigma_A{}^h v_h N_v \exp(-E_A/kT) \qquad (3\text{-}1)$$

where $\sigma_A{}^h$ is the capture cross-section for a hole with velocity v_h by an acceptor with binding energy E_A, and N_v is the effective density of states in the valence band. The radiative recombination rate of free electrons of density n and velocity v_e, with

bound holes is

$$r_{fb} = \sigma_A{}^e v_e n, \tag{3-2}$$

where $\sigma_A{}^e$ is the capture cross-section of the acceptor for an electron. At low temperatures, γ is very small and there is negligible thermal quenching of the luminescence; however, as the temperature is increased, γ increases very rapidly. The temperature at which thermal quenching of the luminescence becomes dominant may be defined as the temperature (T_q) where the two rates γ and r_{fb} become equal. There are two cases to consider:

(a) In conducting crystals, the density of photo-excited electrons is small compared to those thermally released from donor impurities since the conductivity is increased only slightly by intense excitation. The thermal equilibrium free electron concentration is (e.g. Blakemore, 1962)

$$n \simeq (N_D - N_A)/[1 + (2N_A/N_C)\exp E_D/kT]. \tag{3-3}$$

At the low temperatures (~80°K), where the quenching of the luminescence takes place, and with typical acceptor concentrations of 10^{15} to 10^{16} per cm^3, Eq. (3) simplifies to

$$n \simeq (N_D - N_A)(N_c/2N_A)\exp - E_D/kT. \tag{3-4}$$

Thus, equating γ and r_{fb}, one obtains for the quenching temperature

$$T_q = \frac{E_A - E_D}{k} \ln \frac{\sigma_A^e v_e N_c (N_D - N_A)}{2\sigma_A{}^h v_h N_v N_A}, \tag{3-5}$$

where the activation energy is $E_A - E_D$.

(b) In insulating crystals, the dark free electron density is negligible compared to the photo-excited concentration Δn. Now

$$\Delta n = g\tau_n, \tag{3-6}$$

where g is the optical volume generation rate (i.e. the density of electron-hole pairs generated per second by the excitation light), and τ_n is the electron lifetime. Equating γ and r_{fb}, one obtains for the quenching temperature

$$T_q = \frac{E_A}{k} \ln \frac{\sigma_A{}^e v_e g\tau_n}{\sigma_A{}^h v_h N_v}, \tag{3-7}$$

where the activation energy is E_A.

Maeda found activation energies of 136 meV for conducting crystals and 165 meV for insulating crystals. These he equated to E_A and $E_A + E_D$ respectively, rather than $E_A - E_D$ and E_A as required by Eqs. (5) and (7). Thus, the correct interpretation is that the high energy band is a result of free electrons recombining with holes bound at acceptors about 165 meV above the valence band, in agreement with other work (Collins, 1959; Pedrotti and Reynolds, 1960; Colbow, 1966).

3. The Energy Shift of the Edge Luminescence in CdS with Excitation Intensity

Recently Dondas and Yee (1966) observed that the luminescence under D.C. excitation shifted towards higher energies for larger excitation intensity for both the high energy band at 5140 Å and

the low energy band at 5180 Å. However, a much larger change of excitation intensity was required for the high energy band than for the low energy band to obtain an equivalent shift in the position of the peaks of the bands.

In flash excitation experiments, the peak of the afterglow spectrum was observed to move towards longer wavelengths with increasing time after excitation both for GaP (Thomas et al, 1965) and for the low energy band in CdS (Colbow 1966). With D.C. excitation the luminescence was found to shift to higher energies with increased excitation intensity for GaP and for CdS (Gross, Razbirin and Permogorov, 1965; Condas and Yee, 1966). Both effects are expected for pair recombination since donor-acceptor pairs of short separation have larger overlap of the wavefunctions and hence give rise to faster electron-hole recombination. Their resulting light emission occurs at higher energies, given by

$$h\nu = E_G - (E_D + E_A) + e^2/\kappa r \qquad (3\text{-}8)$$

where r, the donor-acceptor separation, is large compared to the electron and hole effective Bohr radii. E_G is the semiconductor band gap, E_D and E_A are the donor and acceptor binding energies, and κ is the static dielectric constant. High D.C. excitation will favor pairs which are closely spaced since the rate of recombination is proportional to the square of the overlap of the wave functions (Colbow, 1965)

$$W = W_o \exp(-2r/r_o) \qquad (3\text{-}9)$$

where W_o is the reaction coefficient, and r_o is the Bohr radius of the less tightly bound carrier.

Following this line of reasoning Condas and Yee concluded that the high energy band in CdS, which showed a shift of about 3.5 meV at 77°K with a 20-fold increase of excitation intensity must also be due to pair recombination. However, this explanation encounters difficulties when one attempts to understand the temperature dependence of the two bands in CdS (Pedrotti and Reynolds, 1960; Gross, Razbirin and Permogorov, 1965; Colbow, 1966). If one were to attribute both bands to pair recombination from different donors to the same acceptor (Gross, Razbirin and Permogorov, 1965), then one is left with that the deeper donor state (giving rise to the low energy band) becomes thermally ionized, thus quenching the luminescence, before the shallower donor (giving rise to the high energy band) does. Secondly, the time resolved spectrum of the afterflow showed no energy shift for the high energy band, but did show one for the low energy band (Colbow, 1966), which supports the view that the high energy band is due to free electron-to-bound hole recombination while the low energy band is due to pair (bound electron-to-bound hole) recombination.

The energy shift as a function of excitation intensity was measured for both bands on several crystals. The energy shift varied by a factor of 3 among different crystals. However, for each crystal the shift of the pair emission was at least 5 times as much as the shift of the free-to-bound emission for the same change in excitation intensity. A typical shift for a 70-fold

increase in excitation intensity was 4 meV for the pair radiation (at $2^{o}K$) and 0.7 meV for the free-to-bound radiation (at $77^{o}K$). The energy shift of the peak of the pair emission, which is dominant at $2^{o}K$, results from the fact that high excitation intensity favors pairs of short separation. The energy shift of the peak of the free-to-bound emission, which is dominant at $77^{o}K$, is shown in Fig. 8 as a function of the mean free electron concentration for crystal F which shows a larger than average shift. The solid line shows a shift proportional to the square root of the free carrier concentration. The latter was calculated from photoconductance measurements under the assumption that, due to rapid capture by defects, carriers do not diffuse from the region of generation.

While the detailed explanation for the energy shift of the free-to-bound transition is not clear at present, two mechanisms are suggested:

(a) Free Carrier Screening

In the presence of a free charge carrier density n, the effective mass Hamiltonian for a shallow impurity (assuming a spherically symmetric mass) is

$$H = -\frac{\hbar^2}{2m^*}\left\{\frac{d^2}{dr^2} + \frac{2}{r}\frac{d}{dr}\right\} - \frac{e^2}{\kappa r}\exp -\frac{r}{\lambda}\,, \qquad (3\text{-}10)$$

where κ is the dielectric constant, and

$$\lambda = (kT\kappa/4\pi ne^2)^{\frac{1}{2}}, \qquad (3\text{-}11)$$

is the Debye-Huckel screening length. A variational calculation can be performed by assuming a trial wave function of the form

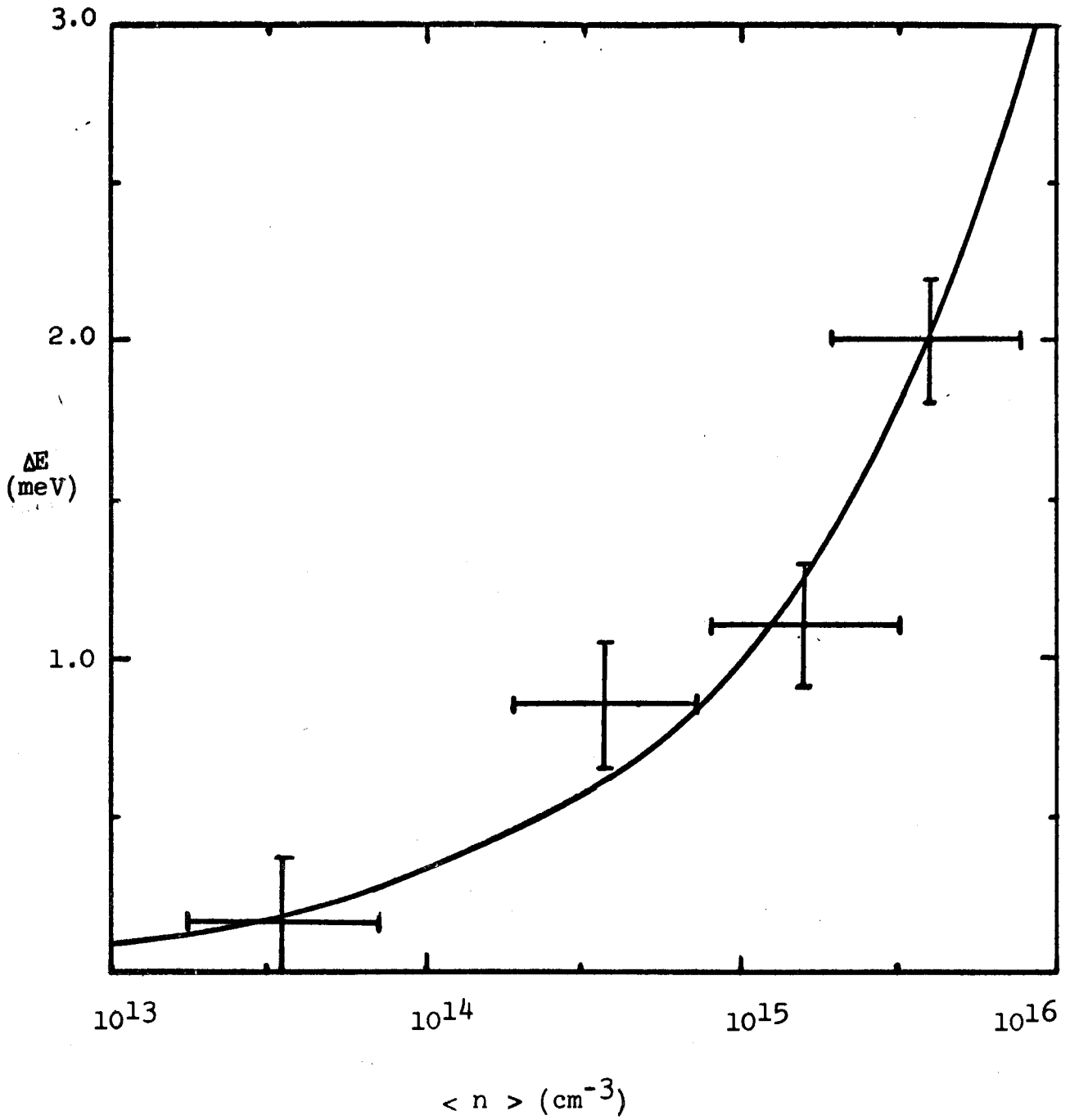

Fig. 8: Energy Shift of the Peak of the Free-to-Bound Emission Band as a Function of the Mean Electron Concentration.

$$\psi = \psi_o \exp(-\alpha r), \tag{3-12}$$

and choosing α so as to minimize the energy

$$E = \int \psi^* H \psi d\tau. \tag{3-13}$$

Introducing the effective Bohr radius,

$$r_o \equiv e^2/2\kappa E_A, \tag{3-14}$$

where E_A is the experimental acceptor binding energy with no screening. Using the dimensionless quantities

$$\beta \equiv r_o/\lambda, \tag{3-15}$$

$$y \equiv 2r_o\alpha, \tag{3-16}$$

and

$$W \equiv E/E_A, \tag{3-17}$$

Eq. (13) then leads to

$$W = y^2/4 - y^3/(y + \beta)^2, \tag{3-18}$$

which has a minimum with respect to y (or α) for

$$y^3 + (3\beta - 2)y^2 + (3\beta^2 - 6\beta)y + \beta^3 = 0 . \tag{3-19}$$

If solved numerically one finds the dependence of acceptor binding energy on free carrier concentration shown in Fig. (9).

For small free carrier density (small β) an approximate solution, neglecting terms in β^2, gives

$$W \simeq 2\beta - 1. \tag{3-20}$$

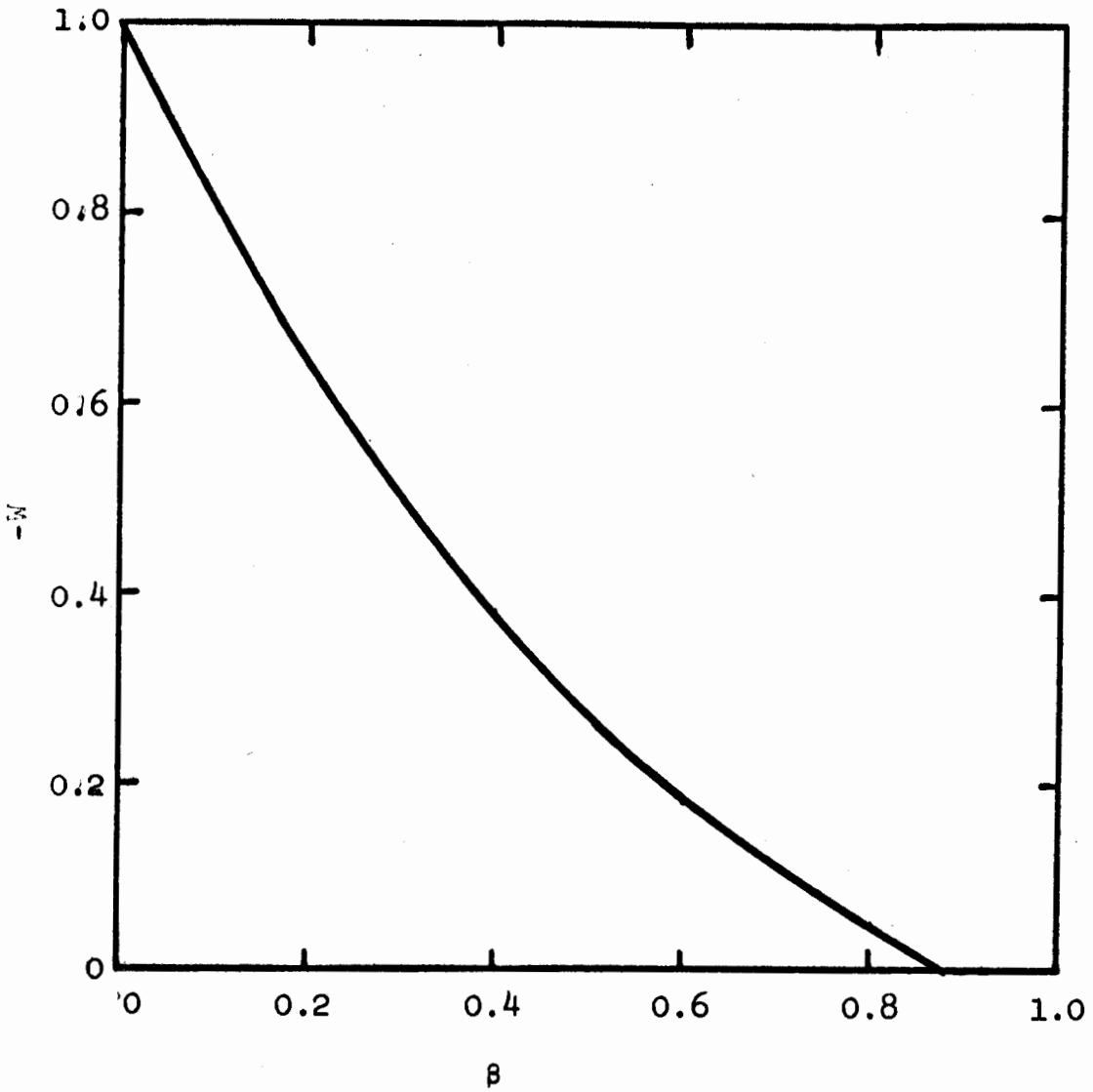

Fig. 9: Dependence of Binding Energy on the Parameter β.

With E_A = 170 meV and κ = 10.33 (Berlincourt et. al., 1963), Eq. (14) leads to a Bohr radius of 4.1 Å. By Eq. (3), the highest free charge carrier density of 3.8×10^{15} per cm^3 at 77^oK will lead to a screening length of 315 Å. Using Eqs. (15) and (20), this leads to a value of $\beta = 0.013$, and a decrease in acceptor binding energy equal to 4.4 meV. This is in reasonable agreement with the observed value of 2.0 meV (Fig. 7). A charge carrier concentration of 4×10^{15} per cm^3 corresponds to 1.2×10^{-6} free carriers inside a Bohr radius of about 4.1 Å. When the free charge carrier density is so low, one may question the validity of the Debye-Huckel screening length approach. However, as an estimate, the calculation appears to give a reasonable answer.

(b) Hot Electron Gas

The rate of the recombination of an electron of kinetic energy E with a bound hole is given by $p_A n v_e \sigma_A^e$ where p_A is the density of the bound holes, n is the density of electrons with energy E and v_e is the electron velocity. Assuming a Boltzmann distribution for a parabolic conduction band, and that the capture cross-section (σ_A^e) is independent of E, the free-to-bound recombination rate becomes,

$$r_{fb}(E) = r_o E \exp(-E/kT_e) \qquad (3\text{-}21)$$

This has a maximum for electrons with a kinetic energy of kT_e. Thus, the peak in the no-phonon emission occurs at

$$E_{fb} = E_G - E_A + kT_e \qquad (3\text{-}22)$$

where E_G is the band gap and E_A is the acceptor binding energy.

At high excitation intensity, the effective electron temperature (T_e) may exceed the lattice temperature (77°K). An electron temperature of 130°K would explain the observed maximum shift of 4 meV. No experimental data are presently available for CdS, and thus it is not known whether 130°K is a reasonable value for the electron temperature.

CHAPTER IV

SURFACE EFFECTS ON PHOTOLUMINESCENCE

1. Introduction

Two types of surface states have been studied in cadmium sulfide. Levine and Mark (1966) have predicted and, using photoconductivity techniques, apparently observed intrinsic surface states. Extrinsic surface states associated with adsorbed impurities (in particular oxygen) have been observed (Bleil and Albers, 1964) to strongly affect exciton emission.

Mark and Levine (1966) derive their theory of intrinsic surface states for ionic crystals using Seitz's (1940) approach to bulk crystal energy states as a starting point. Surface ions are considered equivalent to bulk ions except for their reduced Madelung potential. The result of their analysis is the prediction that surface cadmium ions will produce states in the forbidden band gap just below the conduction band (electron traps), and that the surface sulfur ions will produce states in the forbidden band just above the valence band (hole traps). Their experiments revealed that photogenerated electrons could become localized in surface traps when the surface was free of adsorbed impurities. In addition, there is no electrostatic limitation to the filling of these traps indicating that the electrons are not compensated by a depletion layer but rather that equal numbers of holes and electrons are being trapped on the surface. Since these intrinsic surface states are traps, rather than recombination centers, they will not contribute to recombination of the photogenerated carriers. Many and Katzir

(1967), from pulsed field-effect and surface photovoltage measurements, found that on (0001) faces of CdS, in a vacuum of 10 microns of mercury, there are practically no acceptor-like surface states following prolonged illumination with UV light. They thus conclude that there are no intrinsic surface states; however, their work may not be in disagreement with Mark and Levine (1966) since their measurements would not detect the equal numbers of electron and hole traps observed by Mark and Levine. Reed and Scott (1964) have postulated a set of intrinsic surface electron traps associated with unsaturated covalent bonds. They claim that, under illumination, these states may act as recombination centers.

Non-radiative recombination at the surface seems to be mainly associated with extrinsic surface states due to adsorbed impurities. Many workers (Bube, 1953; Seraphin, 1953; Liebson, 1954, 1955; Auth, 1961; Eckart and Asch, 1961; Reed and Scott, 1964; Mark, 1965b) have observed the effect of various gaseous ambients on the photoconductivity and photoconductive response of CdS crystals, while Bleil and Albers (1964) have observed the influence of ambient atmospheres on the exciton emission of CdS.

A large peak, in the region of the absorption edge, has been observed in the photoconductivity spectral response curves of cadmium sulfide. The response to photons with energy greater than the band gap (i.e. those with higher absorption coefficients) varies markedly with the ambient. Bube (1956) suggests that carriers produced near the surface have a shorter lifetime than those in the bulk, while Winogradoff (1961) proposes that the

fall-off in response at short wavelengths is associated with a reduced quantum yield. Ryvkin and Khansevarov (1958) have shown that different surface treatments cause considerable changes in the shape of the spectral response curve. DeVore (1956) has made a theoretical analysis of the shape of the spectral distribution curves. The analysis is based on the effects of surface and volume recombination on the optically generated free electrons as the excitation wavelength and hence the absorption coefficient is varied. Mark (1965a) has extended this analysis to the case of an insulator with two carriers. These analyses have been extended to the case of an applied electric field in Appendix A. Results similar to the peak observed in the photoconductivity spectral response curve are expected for the photoluminescence spectral response curve. The photoluminescence efficiency was measured as a function of excitation wavelength and the results of this experiment are discussed in the following section. In the third section of this chapter, the effect of a D.C. electric field on the photoluminescence efficiency is described.

The main non-radiative recombination centers on the surface of CdS are probably associated with chemically adsorbed oxygen ions (Williams, 1962). These negative oxygen ions are charge compensated by a depletion layer in the bulk immediately adjacent to the surface. Several workers (Williams, 1962; Mark, 1964; Many and Katzir, 1967) have shown that the oxygen can be removed, by illuminating the crystal with UV light, while the crystal is in an atmosphere of nitrogen, an inert gas, or in vacuum. The

photogenerated holes are swept to the surface (by the strong electric field in the depletion layer), where they neutralize the oxygen ions which are then free to diffuse away from the crystal. After this treatment, there is no evidence of extrinsic surface states and the photoconductive response is high even at short wavelengths. The effect of oxygen photodesorption on the photoluminescence efficiency is described in the third section of this chapter.

The final section of this chapter describes evidence for a new radiative recombination center associated with nitrogen acceptors near the surface. The new emission bands are obtained by heating the crystal briefly in a nitrogen atmosphere and are eliminated by a short etch in concentrated HCl.

2. Luminescence Efficiency as a Function of the Wavelength of Excitation

The object of this experiment, in which the luminescence efficiency is measured as a function of excitation wavelength (i.e. optical absorption coefficient), is to determine the effect of non-radiative surface recombination on the luminescence efficiency. Higher energy photons are absorbed closer to the surface than photons of energy near the band gap, and thus a larger fraction of the free holes can drift and/or diffuse to the surface. At the surface, there are usually non-radiative recombination centers associated with adsorbed oxygen ions.

Fig. (10) shows the results of measuring the relative luminescence efficiency as a function of the wavelength of the excitation

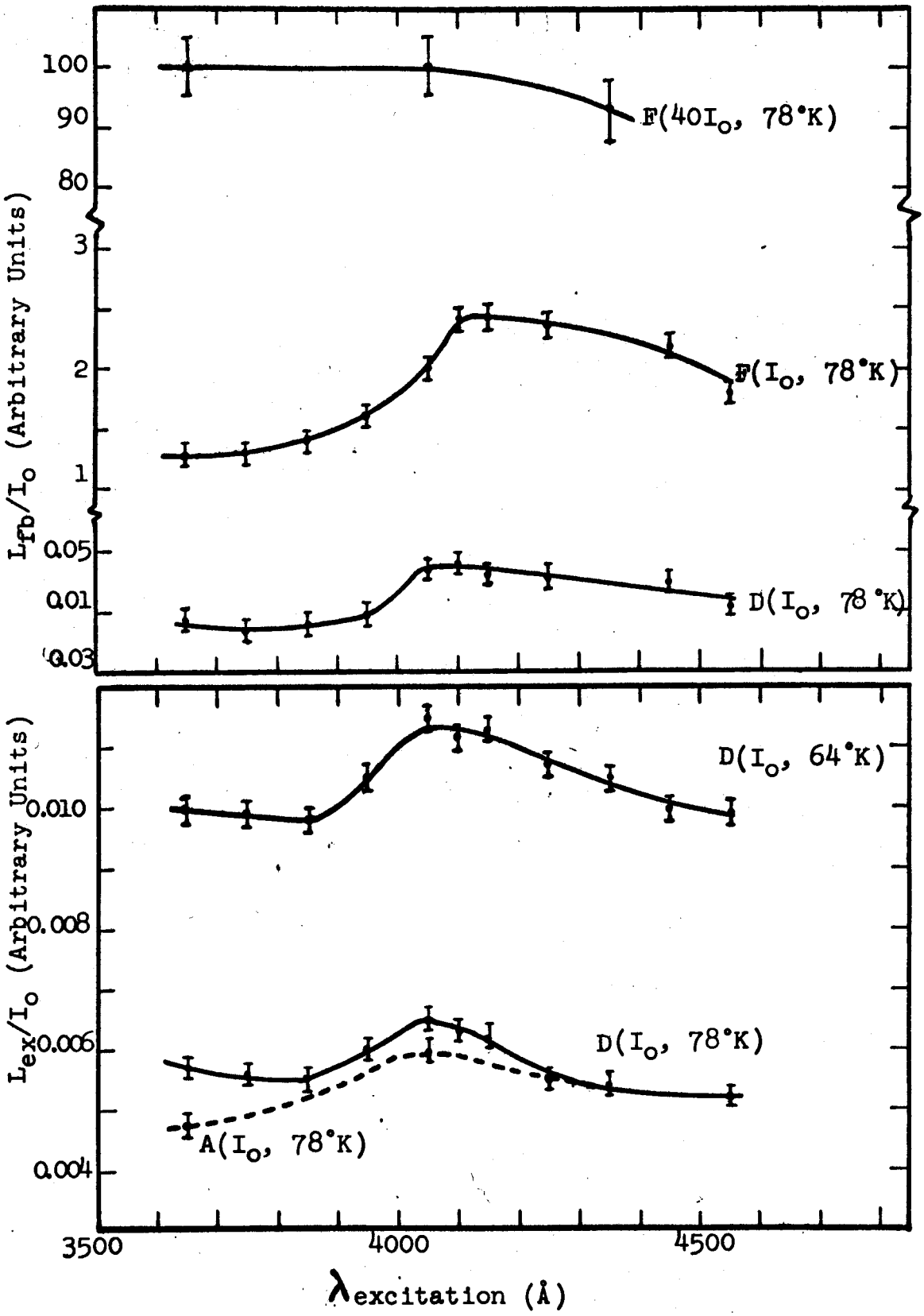

FIG. 10: RELATIVE PHOTOLUMINESCENCE PER ABSORBED PHOTON AS A FUNCTION OF EXCITATION WAVELENGTH

light for two crystals, a high-resistivity ($\rho > 10^8$ ohm-cm at 295°K) platelet (F) grown by the method of Frerich (1947), and a low-resistivity ($\rho \sim 10$ ohm-cm at 295°K) crystal (D) cut from a large single crystal obtained from the Clevite Corporation. The platelets grow with their flat surface perpendicular to the $(11\bar{2}0)$ axis and this surface contains equal numbers of sulfur and cadmium atoms in a checkerboard array (Levine and Mark 1966). After etching, crystal D showed a shiny surface made up of sulfur atoms, and a dull opposite surface made up of cadmium atoms (Markelois et al., 1962). The luminescence from the sulfur side was brighter than that from the cadmium side; the data shown for crystal D is for the sulfur side.

The striking feature of the curves in Fig. (10) is that the shape of the curve is approximately temperature-independent, and is similar for the exciton emission and the free-to-bound emission. In the cases shown, the efficiency is peaked for an excitation wavelength at about 4050 Å. This wavelength corresponds to an energy appreciably greater than the energy band and corresponds to no known structure in these bands.

To understand these data we have assumed that diffusion of carriers into the interior of the crystal does not take place, but rather that the photo-excited carriers are spread over an average distance, $1/\alpha$, where $1/\alpha$ is the optical absorption length. This assumption is justified by the analysis in Ch. VI, where the hole lifetime is shown to be very short. Once the holes become bound, the electrons are prevented from diffusing out of the photo-excited region by space-charge fields. The

fall-off in efficiency at short excitation wavelengths is attributed to non-radiative recombination at extrinsic surface states associated with adsorbed oxygen ions. This recombination is aided by the electric field in the depletion layer adjacent to the surface, which drives holes to the surface. With short wavelength excitation a greater fraction of the photogenerated holes can reach the surface. The effect of the surface is less pronounced at higher excitation intensity, as shown in the curve labelled $40I_o$ in Fig. (10), where the excitation intensity is 40 times higher than that used in obtaining the other curves. Apparently the electric field is screened out in the interior of the crystal at high carrier densities.

The drop in luminescence efficiency at wavelengths longer than 4050 Å is attributed to the decrease in carrier density as the carrier generation rate density (αI_o) decreases. The relevant photoluminescence efficiency should then be defined as luminescence per volume generation rate (αI_o) rather than luminescence per total incident flux (I_o). This has been plotted in Fig. (11), using the optical absorption coefficient reported by Hall (1956). The peak in the efficiency curve at 4050 Å is now removed. No clear differences have been established for the three types of surfaces studied.

For crystal A, the bulk properties of which are analyzed in detail in Ch. V and VI, only slight non-radiative surface recombination was found. This is interpreted as meaning that the extrinsic surface state density was low.

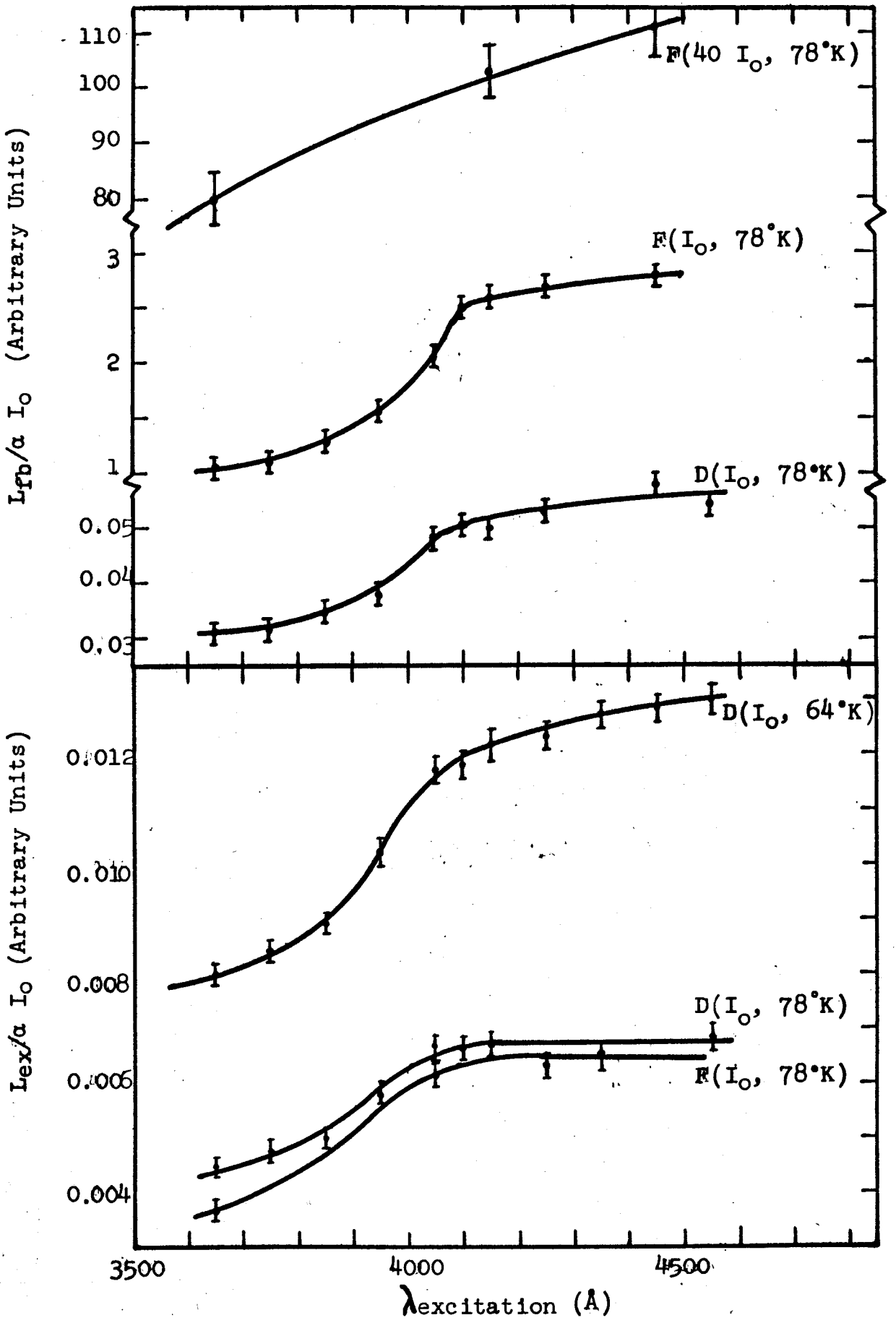

FIG. 11: RELATIVE PHOTOLUMINESCENCE PER AVERAGE VOLUME EXCITATION INTENSITY AS A FUNCTION OF EXCITATION INTENSITY

As a general rule it proved difficult to obtain reproducible results in this experiment. One of the reasons is believed to be that the extrinsic surface state density may change slowly with time and also vary markedly from crystal to crystal. The extrinsic surface state density may also depend strongly on the method of preparing the crystal for the experiment.

3. The Effect of an Electric Field and of Oxygen Photodesorption on the Luminescence

The luminescence efficiency can be increased by removing the electric field at the surface through oxygen photodesorption, or by applying an external electric field to counteract the negative surface field, thus preventing holes from being drawn to the surface.

The effect of applying a D.C. electric field perpendicular to the illuminated surface is shown in Fig. (12) for the emission band at 5140 Å for crystal F at 78°K. Qualitatively similar results were found for the other crystals measured. The luminescence decreases when the illuminated surface is negative and increases or is unchanged when the illuminated surface is positive. The field enhancement of the luminescence is strong when a large built-in field exists near the surface (bands bent up). Oxygen photodesorption or large excitation intensity will straighten the bands and thus reduce the enhancement effect of applying a positive voltage to the illuminated surface. Once the bands are level near the surface, the conduction electrons will prevent a positive field from bending the bands down and thus from further

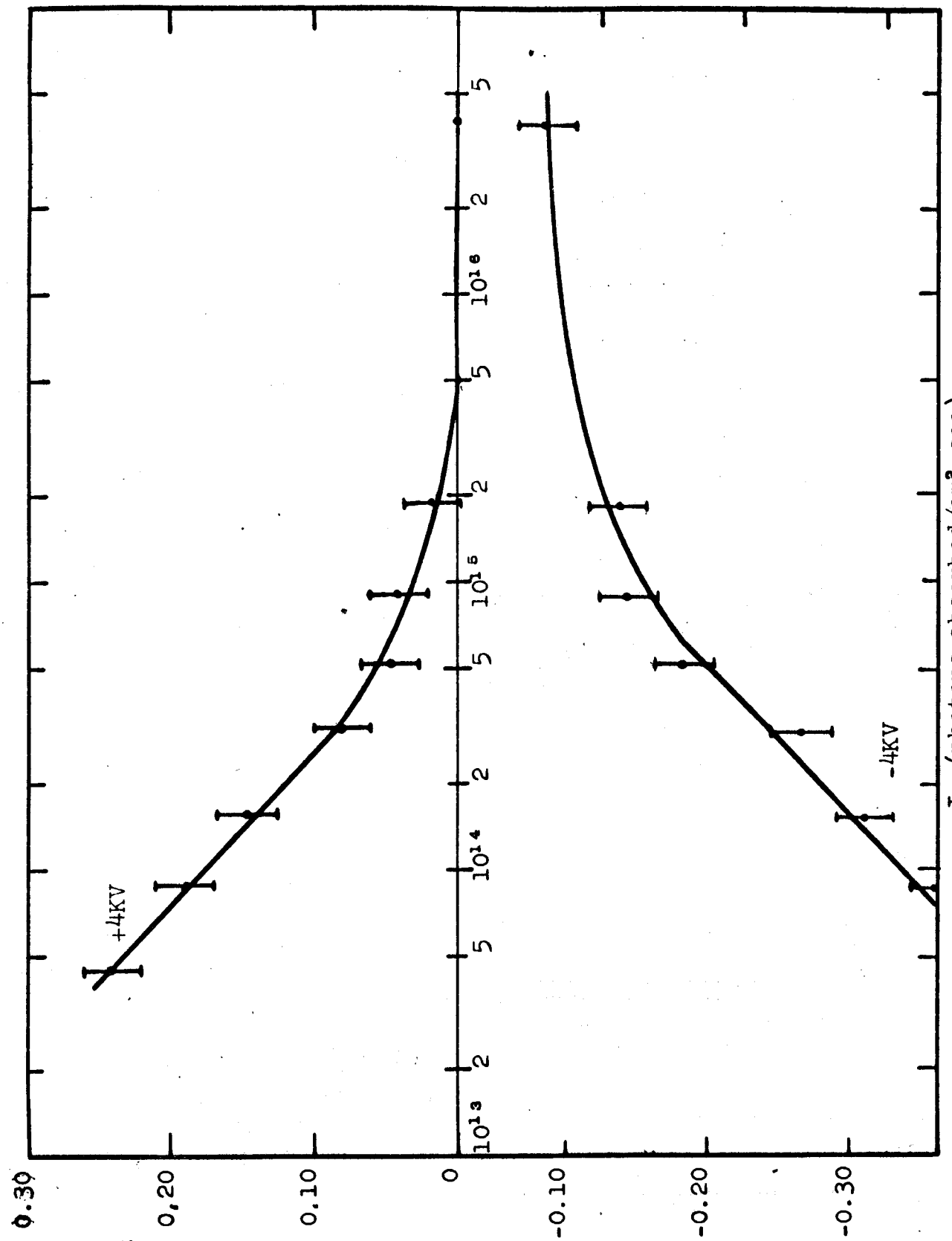

FIG. 12: EFFECT OF A D.C. ELECTRIC FIELD ON THE PHOTOLUMINESCENCE

enhancing the luminescence. A negative field will bend the bands up further, thus causing more holes to be lost at the surface. At low excitation, the field quenching is larger since the region near the surface has a larger resistivity than for higher excitation and thus a larger fraction of the applied voltage will be effective in sweeping holes to the surface. No quantitiative analysis is attempted since only external voltages are measurable and the internal field distribution is not.

In the oxygen photodesorption experiment the chemically adsorbed oxygen is removed from the surface, resulting in enhancement of the luminescence. Exposure to the atmosphere decreased the luminescence again, apparently as a result of readsorption of the oxygen.

4. Photoluminescence Associated with Nitrogen Impurities

(a) Introduction

The main features of the luminescence spectrum of CdS are now well understood. Most crystals show two broad bands at low temperatures near 5135 and 5180 Å, which are repeated at longer wavelengths through the simultaneous emission of one or more longitudinal optical phonons (LO). These bands are caused by the recombination of a free electron with a bound hole (f-b) and a bound electron with a bound hole (b-b) respectively (Pedrotti and Reynolds, 1963; Colbow, 1966). The electrons are usually bound to donors 30 meV below the conduction band, and the holes to acceptors 170 meV above the valence band (Colbow, 1966). The donors may be associated with foreign

impurities (e.g. Al, Cl) or possibly defect centers, while the acceptors are most likely due to cadmium vacancies (Woodbury, 1964; Handelman and Thomas, 1965). We have been able to observe both free-to-bound and bound-to-bound recombination radiation associated with a new acceptor level 131 meV above the valence band due to nitrogen impurities.

(b) Theory

When an electron bound to a donor recombines with a hole bound to an acceptor a distance r from the donor, the energy of the emitted light is (Thomas et al., 1964)

$$E_{bb} = E_G - (E_A + E_D) + e^2/\kappa n - nE_p \quad . \qquad (4\text{-}1)$$

Here E_G is the band-gap energy, E_A and E_D the acceptor and donor binding energies respectively, $e^2/\kappa r$ is the Coulomb energy between the hole and the electron, and κ is the static dielectric constant. The energy nE_p represents the simultaneous emission of n (= 0, 1, 2, ...) longitudinal optical phonons of energy E_p.

For the radiative transition of a free electron to a neutral acceptor, the energy of the emitted light is (Colbow, 1966)

$$E_{fb} = E_G - E_A + E_k - nE_p \qquad (4\text{-}2)$$

where $E_k \simeq kT$ is the kinetic energy of the free electron. At 2^oK, the kinetic energy of the electron is negligible, and the acceptor binding energy is readily calculated from the observed energy of the free-to-bound no-phonon emission peak and the energy gap of the material.

(c) Experimental and Discussion

Fig. 13 shows the free-to-bound and bound-to-bound recombination radiation which is usually observed from a high-purity CdS crystal under D.C. excitation with highly absorbed excitation light. At 2°K, both the f-b (5135 Å) and the b-b (5180 Å) are observed, while at 64 and 78°K the shallow donor becomes ionized and only the f-b transition can be seen. After heating the crystal for a few seconds in a nitrogen ambient, the spectrum shown in Fig. 14 results. At 2°K, two new bands appear at 5050 and 5100 Å, which we attribute to f-b and b-b transitions respectively, involving nitrogen acceptors. At the highest temperatures, the 5100 Å band disappears as in Fig. 13 due to ionization of the shallow donor. The nitrogen acceptors and the cadmium vacancy acceptors differ in binding energy by 38.5 meV. This is about the same magnitude as the LO phonon energy (38.1 $\pm$ 0.5 meV from Fig. 16), with the result that the phonon replicas of the transitions to the nitrogen acceptor are masked by the transitions involving the cadmium vacancy acceptors. The spectra at 64 and 78°K in Fig. 14 show that the free-to-bound transition to the nitrogen acceptor decreases with increasing temperature relative to the free-to-bound transition to the cadmium vacancy acceptor. This is expected since with increasing temperature the shallower nitrogen acceptors will become ionized sooner. The energy level scheme showing the f-b and b-b no-phonon transitions is shown in Fig. 15.

Using time-resolved spectroscopy (Colbow, 1966), it was possible to look just at the afterglow between 100 and 600 μ sec

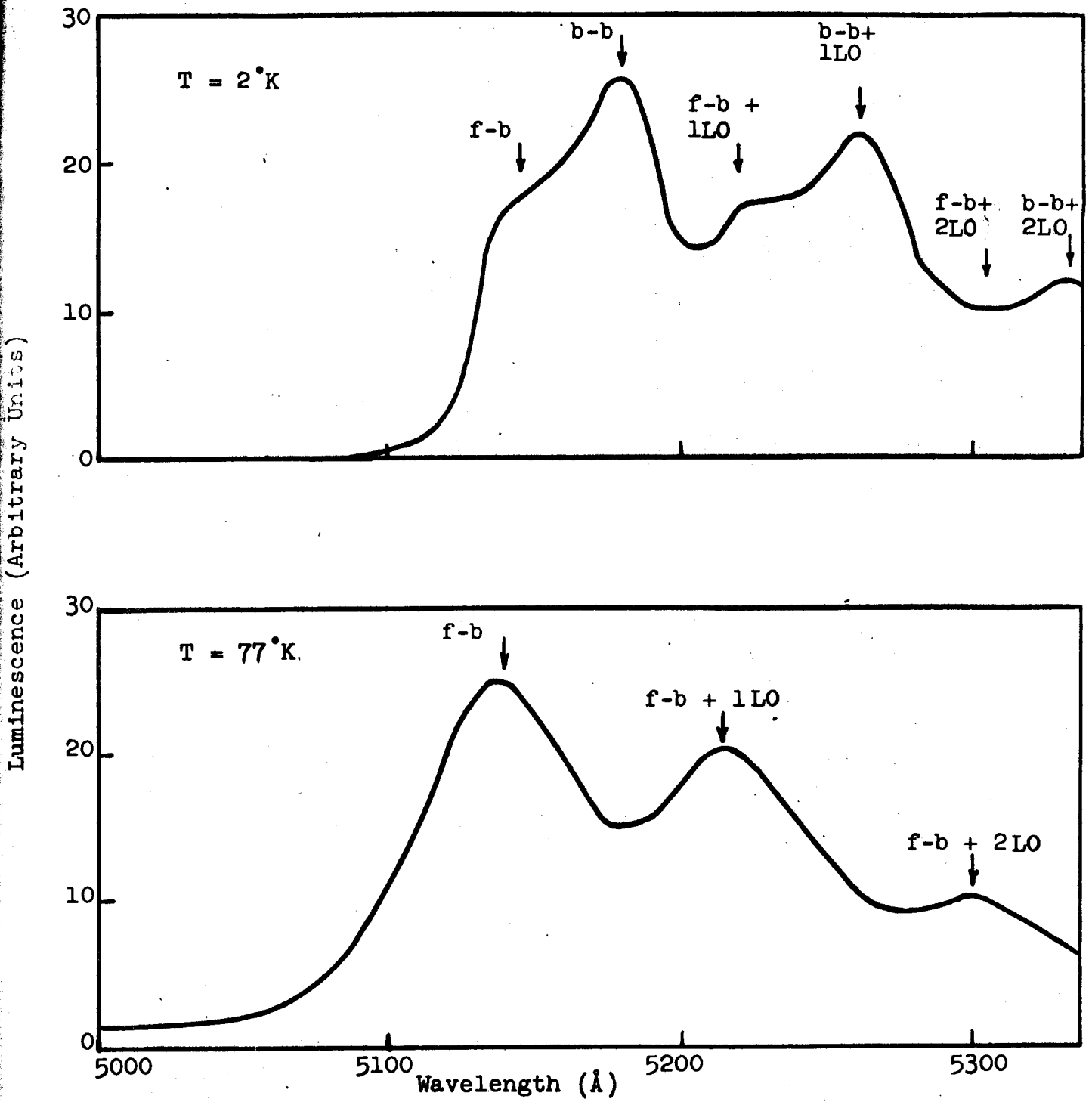

FIG. 13: THE FREE-TO-BOUND AND BOUND-TO-BOUND RECOMBINATION RADIATION UNDER DC EXCITATION OF AN ETCHED HIGH-PURITY CdS CRYSTAL

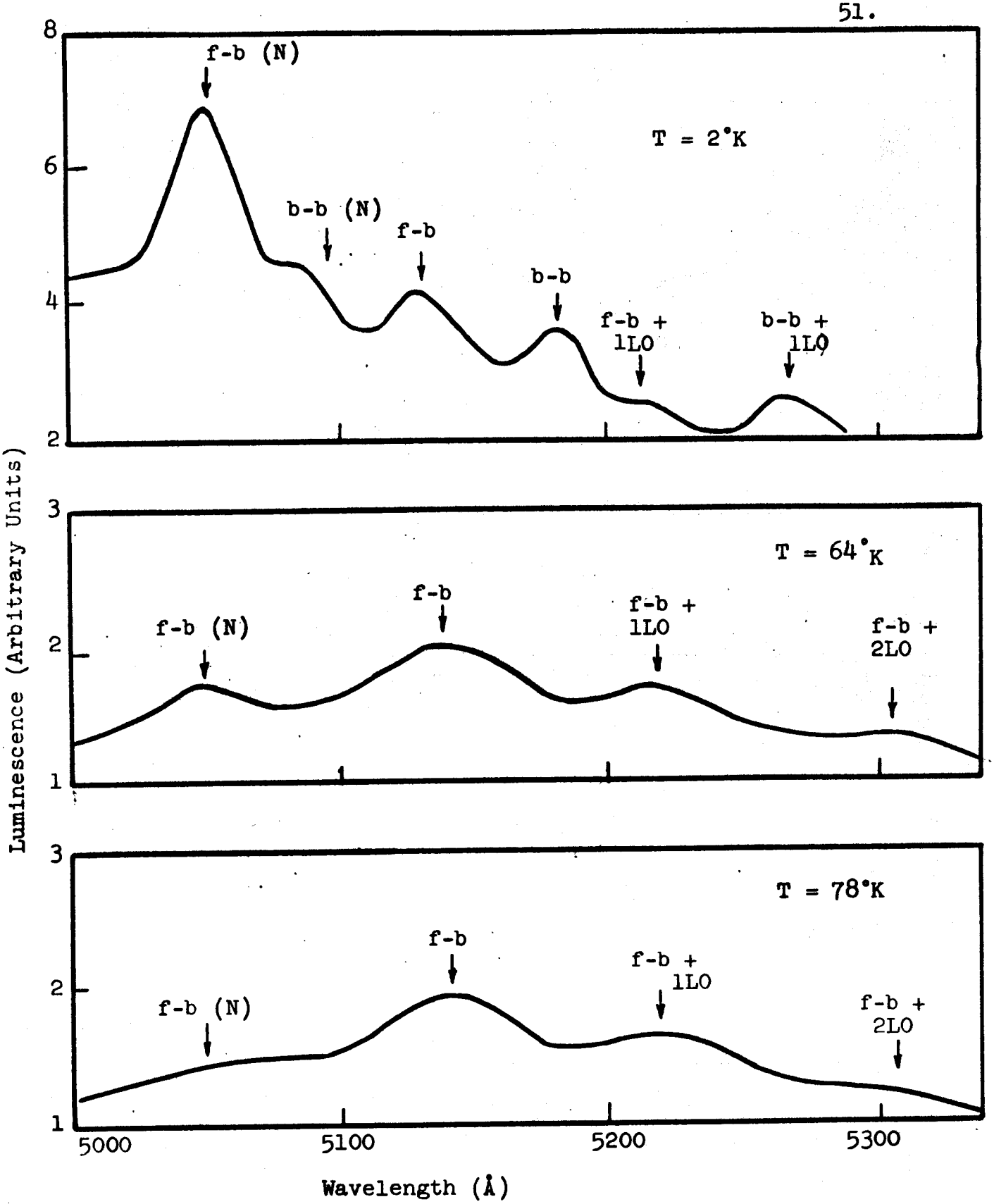

FIG. 14: THE FREE-TO-BOUND AND BOUND-TO-BOUND RECOMBINATION RADIATION UNDER DC EXCITATION OF A HIGH-PURITY CdS CRYSTAL PREVIOUSLY HEATED IN A NITROGEN AMBIENT

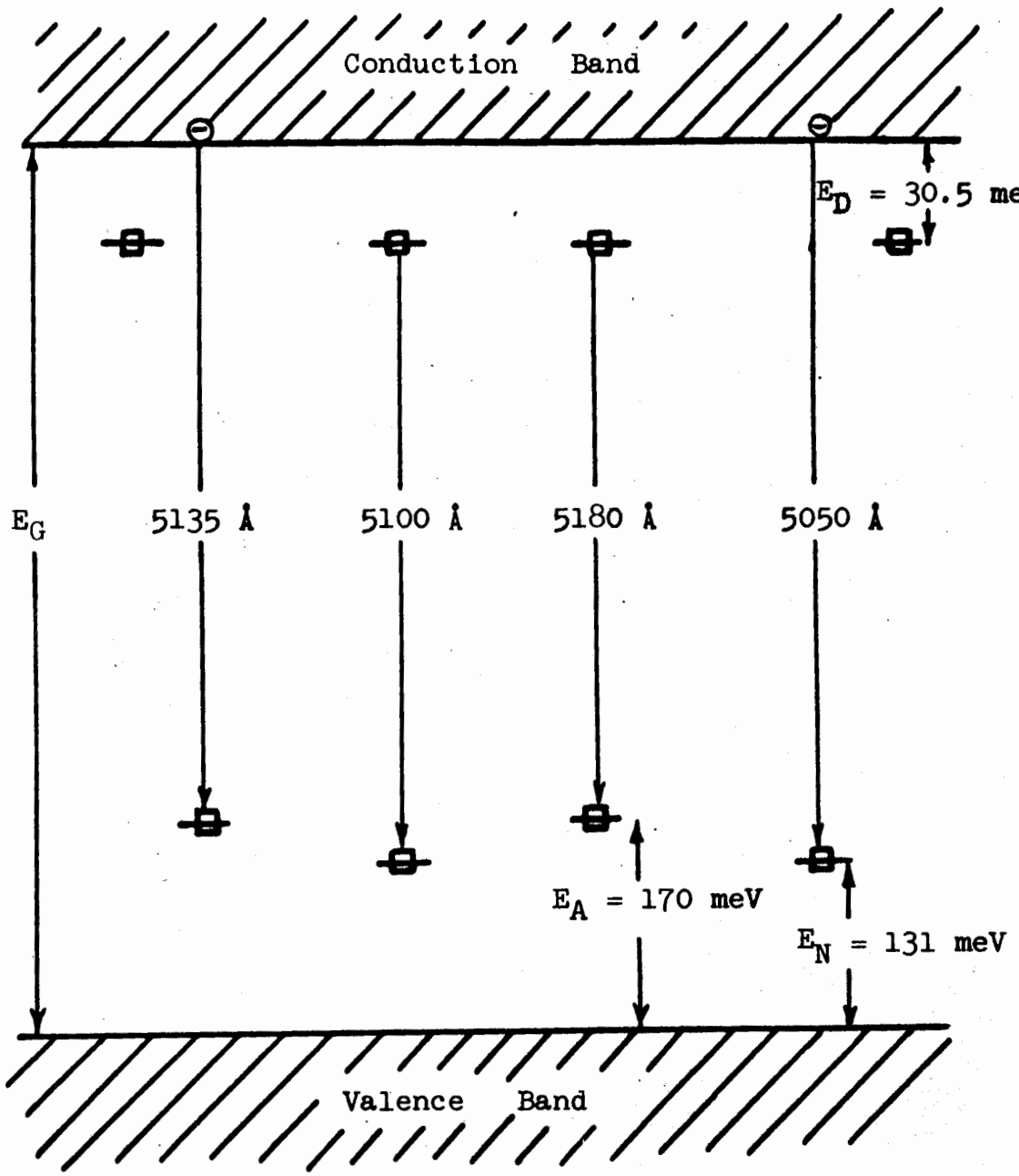

FIG. 15: ENERGY BAND DIAGRAM SHOWING THE NO-PHONON TRANSITIONS OF FIGS. 13 AND 14

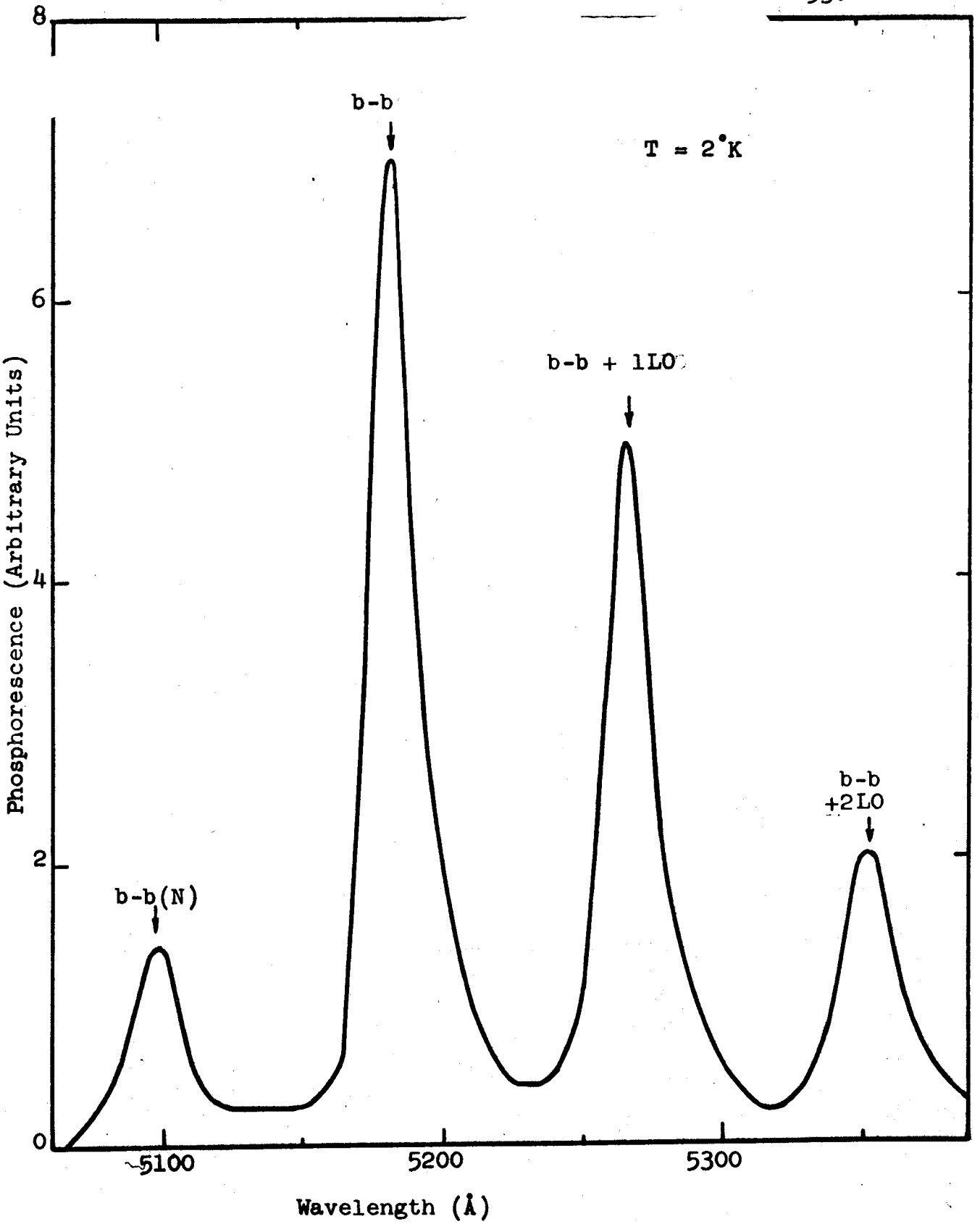

FIG. 16: PHOSPHORESCENCE SPECTRUM 100 TO 600 μSEC AFTER EXCITATION OF A HIGH-PURITY CdS CRYSTAL PREVIOUSLY HEATED IN A NITROGEN AMBIENT

after the start of the pulse of excitation light. The exciton and the free-to-bound radiation have died out 100 microseconds after excitation and one obtains only the bound-to-bound transitions (Fig. 16). The transition involving the nitrogen acceptor (5098 Å) is less intense in the afterglow than the transition involving the cadmium vacancy acceptor, while the reverse was true under D.C. excitation (Fig. 14). This is expected since the nitrogen acceptor has the smaller binding energy and thus the larger Bohr radius. This means a larger wavefunction overlap with neighboring donors and thus a larger recombination rate (Colbow, 1965), which in turn implies a faster decay of the afterglow and a higher intensity under D.C. excitation.

Heating the crystal for a few seconds in a nitrogen or air ambient to the point where the crystal turns red, produces the bands associated in Figs. 14 and 16 with the nitrogen acceptors. Subsequent etching for about 10 to 30 seconds in concentrated HCl removes them again, suggesting that the nitrogen diffused only a "short" (i.e. of the order of microns) distance into the crystal. Heating the crystal in an oxygen atmosphere did not produce any new bands in addition to those observed in Fig. 13, but reduced the overall efficiency. The latter was attributed to increased non-radiative surface recombination because of a strong electric field due to adsorbed oxygen (Ch. IV).

"Prolonged" heating (i.e. for 2 or 3 minutes) in either nitrogen or oxygen will first cause the free exciton emission to decrease and finally disappear and the f-b and b-b bands with the phonon replicas are broadened until they merge into a

continuous band which then decreases in intensity. These effects are again attributed to strong electric fields near the surface due to chemi-sorbed oxygen ions (Ch. IV).

CHAPTER V

BOUND ELECTRON-TO-BOUND HOLE AND EXCITON RECOMBINATION KINETICS

1. Theory

In this chapter, the luminescence efficiency of the bound electron-to-bound hole emission band and the exciton emission lines are considered.

At temperatures below about $35^{o}K$, the photo-generated electrons and holes are rapidly captured by the donors (N_D) and the cadmium vacancy acceptors (N_A) respectively, and the recombination of bound holes with bound electrons becomes important. When an electron bound to a donor recombines with a hole bound to an acceptor, a distance r from the donor, the energy of the emitted light is (Thomas et al, 1964)

$$E_{bb} = E_G - (E_A + E_D) + e^2/\kappa r - nE_p. \qquad (5\text{-}1)$$

Here E_G is the band gap energy, E_A and E_D the acceptor and donor binding energies respectively, $e^2/\kappa r$ is the coulomb energy between the ionized donor and acceptor, and κ is the static dielectric constant. The energy nE_p represents the simultaneous emission of $n(= 0, 1, 2, ...)$ longitudinal optical phonons of energy E_p. The bound-to-bound emission band is fairly broad and this accounted for in part by the variation in the coulomb energy term for pairs of various separations. Additional broadening occurs due to interaction of the trapped carriers with the lattice with the consequent absorption or emission of transverse

optical and acoustical phonons (Colbow, 1966).

For an isolated neutral donor-acceptor pair of separation r, the rate of recombination between the bound electron and the bound hole is proportional to the square of the overlap of the wave functions (Colbow, 1965),

$$W = W_o \exp(-2r/r_o), \tag{5-2}$$

where W_o is the reaction coefficient, and r_o is the Bohr radius of the less tightly bound carrier, which for E_D less than E_A is the electron. The Bohr radius may be obtained through the hydrogenic energy equation

$$E_D = e^2/2\kappa r_o \, . \tag{5-3}$$

Since the ionized donors and acceptors have coulomb attractive capture cross-sections, they are expected to trap most of the free electrons and holes very rapidly before they can reach a non-radiative recombination center or the surface. Once the carriers are trapped at the donor and acceptor sites, the only probable process is the bound-to-bound radiative recombination transition. The efficiency of the bound electron-to-bound hole emission is expected to vary only slowly as the excitation intensity is increased since closely spaced pairs are able to recombine very fast (Eq. 2).

The steady-state radiative recombination rate for free excitons may be obtained from the rate equation

$$dN/dt = 0 = knp - N/\tau_r - N/\tau_n + CN \exp(-\epsilon/kT), \tag{5-4}$$

where N is the density of excitons, knp is the formation rate from free electrons and holes, τ_r and τ_n are the radiative and non-radiative lifetimes, and CNexp($-\epsilon/kT$) represents the thermal ionization rate of excitons bound with energy ϵ. The radiative recombination rate is then

$$N/\tau_r = knp/(1 + \tau_r/\tau_n + C\tau_r \exp -\epsilon/kT), \tag{5-5}$$

which for fixed temperature should depend on the product of the free carrier densities. Neglecting variations in k, τ_r and τ_n with excitation intensity, Eq. (5) may be written as

$$N/\tau_r = Rnp, \tag{5-6}$$

where the constant R is

$$R = k/(1 + \tau_r/\tau_n + C\tau_r \exp -\epsilon/kT). \tag{5-7}$$

The total exciton emission is then

$$L_{ex} = R \int_o^\infty npdx \ . \tag{5-8}$$

For the case where the current gradients may be neglected (see Ch. VI, Eqs. 5 and 7), the exciton emission efficiency is

$$\eta_{ex} = L_{ex}/I_o = R\langle p\tau_n \rangle, \tag{5-9}$$

where

$$\langle p\tau_n \rangle = \int_o^{1/\alpha} \alpha p\tau_n \exp(-\alpha x)dx. \tag{5-10}$$

2. Data

Data on two crystals are reported in this chapter and are representative of measurements made on several "high-purity" CdS crystals. These crystals are not intentionally doped and the impurity concentration is probably less than 10^{16} per cm^3 (Colbow, 1966). Crystal A is a high-resistivity platelet grown by the method of Frerich (1947), while D is a high-conductivity crystal cut from a large single crystal obtained from the Clevite Corporation.

The relative bound-to-bound emission efficiency as a function of excitation intensity is shown in Fig. (17) for crystal A at $2^{o}K$. A similar curve is obtained for crystal D. Fig. (18) shows the relative emission of the free exciton "A" for crystals A and D at 64 and $78^{o}K$. Also shown are the bound exciton emissions (I_1 and I_2) at $2^{o}K$.

3. Discussion

For crystal A at $2^{o}K$, the main emission is the bound electron-to-bound hole recombination at 5180 Å. The emission efficiency of this band (Fig. 17) showed only the expected slow variation with excitation intensity over several decades of excitation intensity (10^{12} to $4 \times 10^{16}/cm^2$-sec).

At high excitation intensities ($I_o > 2 \times 10^{15}$ photons/cm^2-sec), the luminescence efficiency of the bound-to-bound emission band decreases (Fig. 17), while the efficiency of the free-to-bound emission band was observed to increase (data not shown). These results may be interpreted as follows: At high excitation

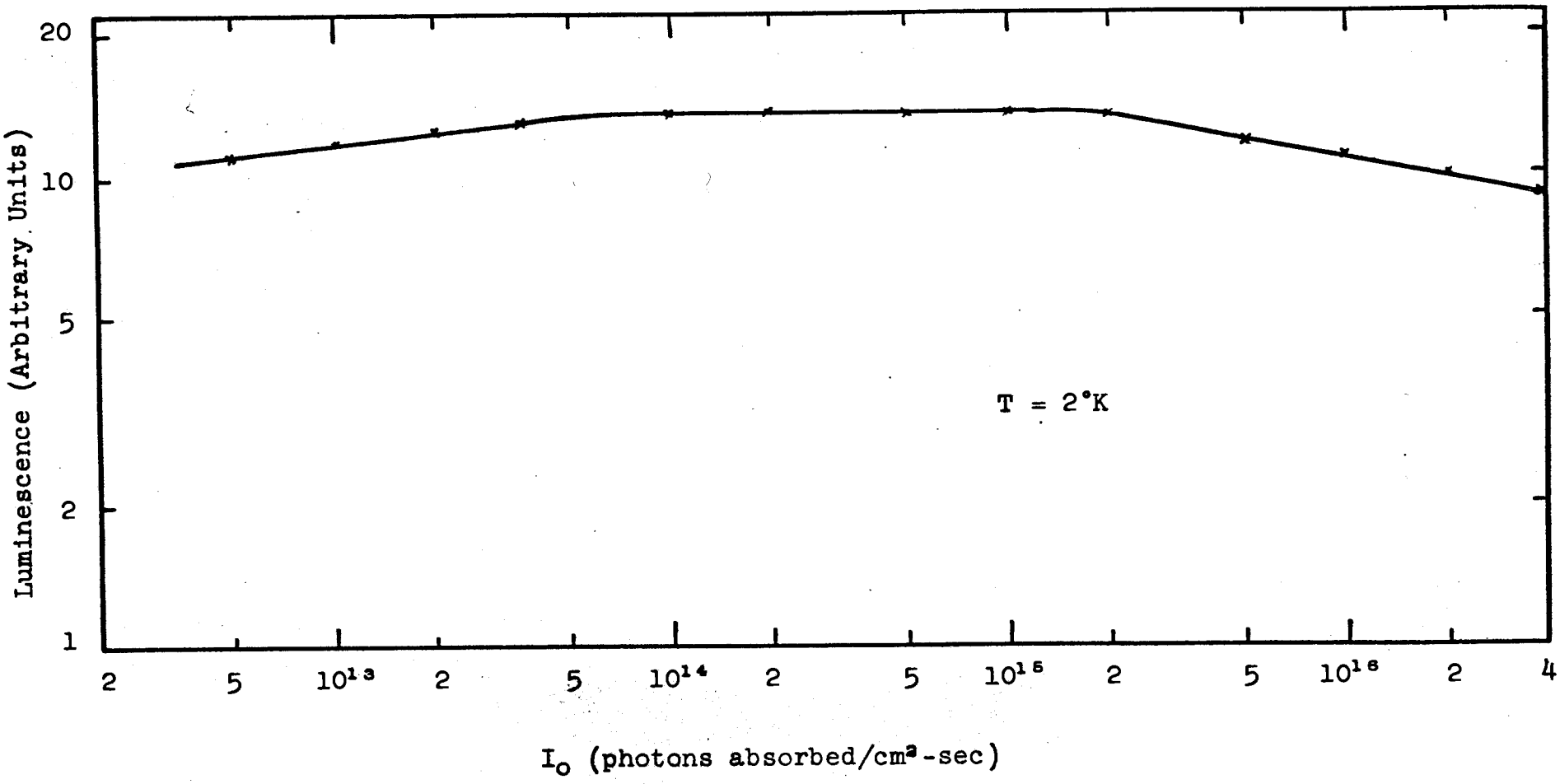

FIG. 17: BOUND-TO-BOUND EMISSION EFFICIENCY AS A FUNCTION OF EXCITATION INTENSITY

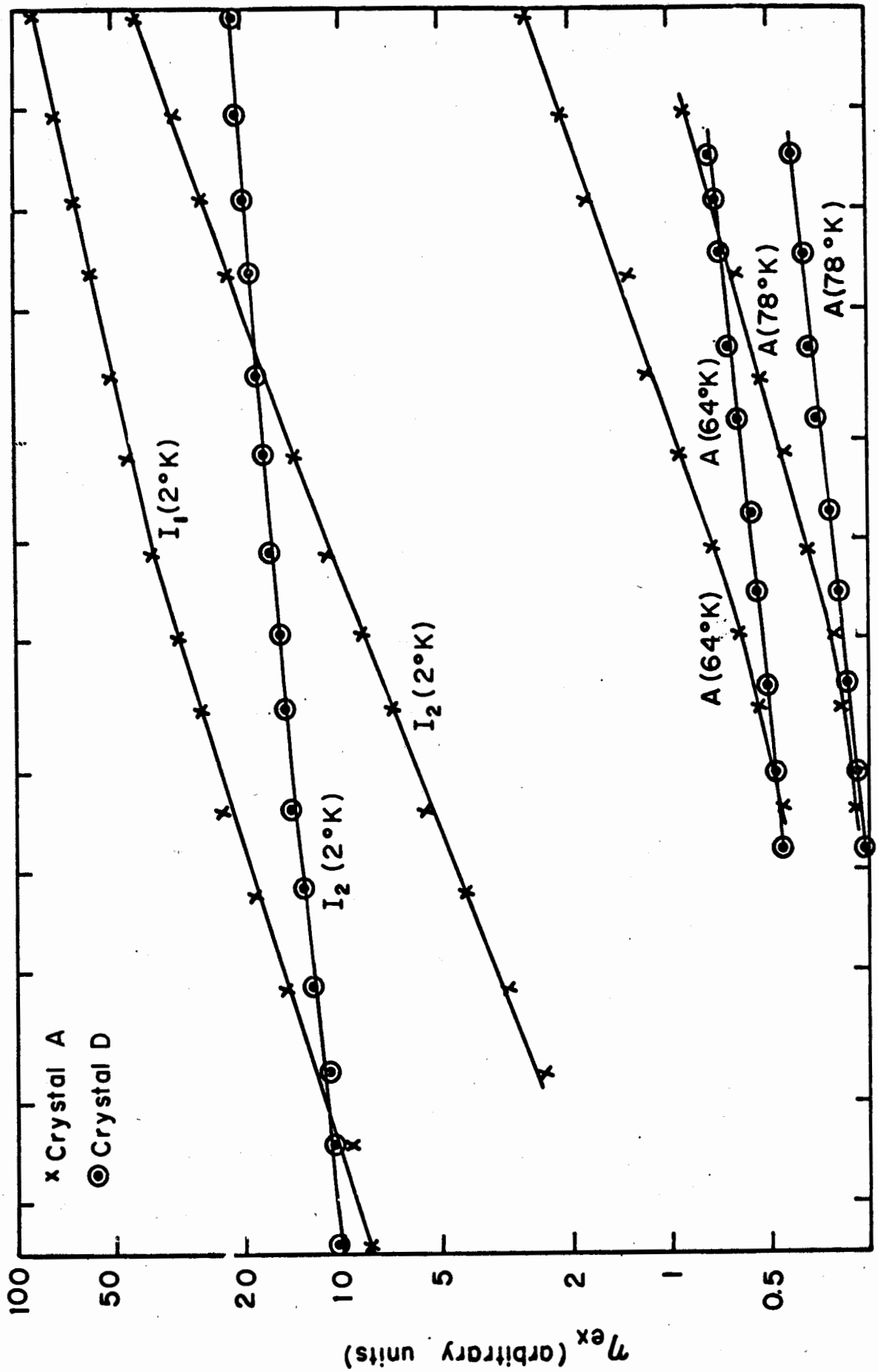

FIG. 18: EXCITON EMISSION EFFICIENCY AS A FUNCTION OF EXCITATION INTENSITY

intensities, the volume excitation rate ($\alpha I_o > 2 \times 10^{20}/cm^3$-sec) is comparable with the volume bound-to-bound recombination rate. The result is that not all of the photo-generated electrons are captured by the donors since a fraction of the donors are already occupied with previously captured electrons. The free electrons which are not captured by the ionized donors are then free to form excitons or recombine with bound holes.

At low excitation intensity, the efficiency drops slightly and this effect may be attributed to the non-radiative recombination of carriers at the surface enhanced by the electric field in the bulk adjacent to the adsorbed oxygen ions (Chapter IV). At higher excitation intensity the electric field is screened from the bulk by the free electron density and holes are no longer swept to the surface.

The formation of free excitons is expected to depend on the product of the free electron and hole densities (Eq. 9). Crystal D has a large thermal electron concentration and thus the total electron concentration will show a slower variation with excitation intensity than for crystal A. This in turn leads to a slower increase in the free exciton emission efficiency with increasing excitation intensity, as observed (Fig. 18). Cooling the crystals from 78 to 64°K increases the free exciton emission (Bleil and Broser, 1964). The emission from excitons bound to neutral acceptors (I_1) (Thomas and Hopfield, 1962) is absent in crystal D. This is in agreement with the work of Handelman and Thomas (1965) who found that crystals can be reproducibly changed from conducting to insulating by controlled

heating in vacuum and cadmium vapor respectively. They conclude that conducting crystals have a much lower density of cadmium vacancy acceptors than high resistivity crystals. The emission from excitons bound to neutral donors (I_2) (Thomas and Hopfield, 1962) is present in both crystals and is roughly of equal intensity. This is expected under the assumption that the donor concentrations (foreign impurities) are similar for all three crystals which were not intentionally doped.

CHAPTER VI

FREE ELECTRON-TO-BOUND HOLE RECOMBINATION KINETICS

1. Theory

The green emission bands are successfully accounted for by N_D donors (foreign impurities), 30 meV below the conduction band, and N_A acceptors (cadmium vacancies), 170 meV above the valence band (Colbow, 1966). To account for the experimental data on luminescence efficiency, it is necessary to introduce, in addition, an effective bulk recombination center of density N_r. Non-radiative surface recombination is not considered in this section.

The assumed energy band model and the relevant transitions are shown in Fig. (19). Here n and p are the densities of free electrons and holes, and n_D, p_r and p_A are the densities of electrons and holes occupying the levels. The capture cross-sections are indicated by σ with the subscript indicating the level and the superscript the type of carrier being captured. The carrier generation rates g, ϵ, and γ represent optical generation, thermal generation of electrons, and thermal generation of holes respectively.

In this section we shall only be concerned with the theory for the temperature range from 60 to 100°K. In this temperature range, the bound electron-to-bound hole (b-b) recombination is unimportant since all donors are ionized, bound exciton recombination is not present since the excitons are all ionized, and the free exciton recombination radiation (while present) is negligible compared to the free electron-to-bound hole (f-b) recombination.

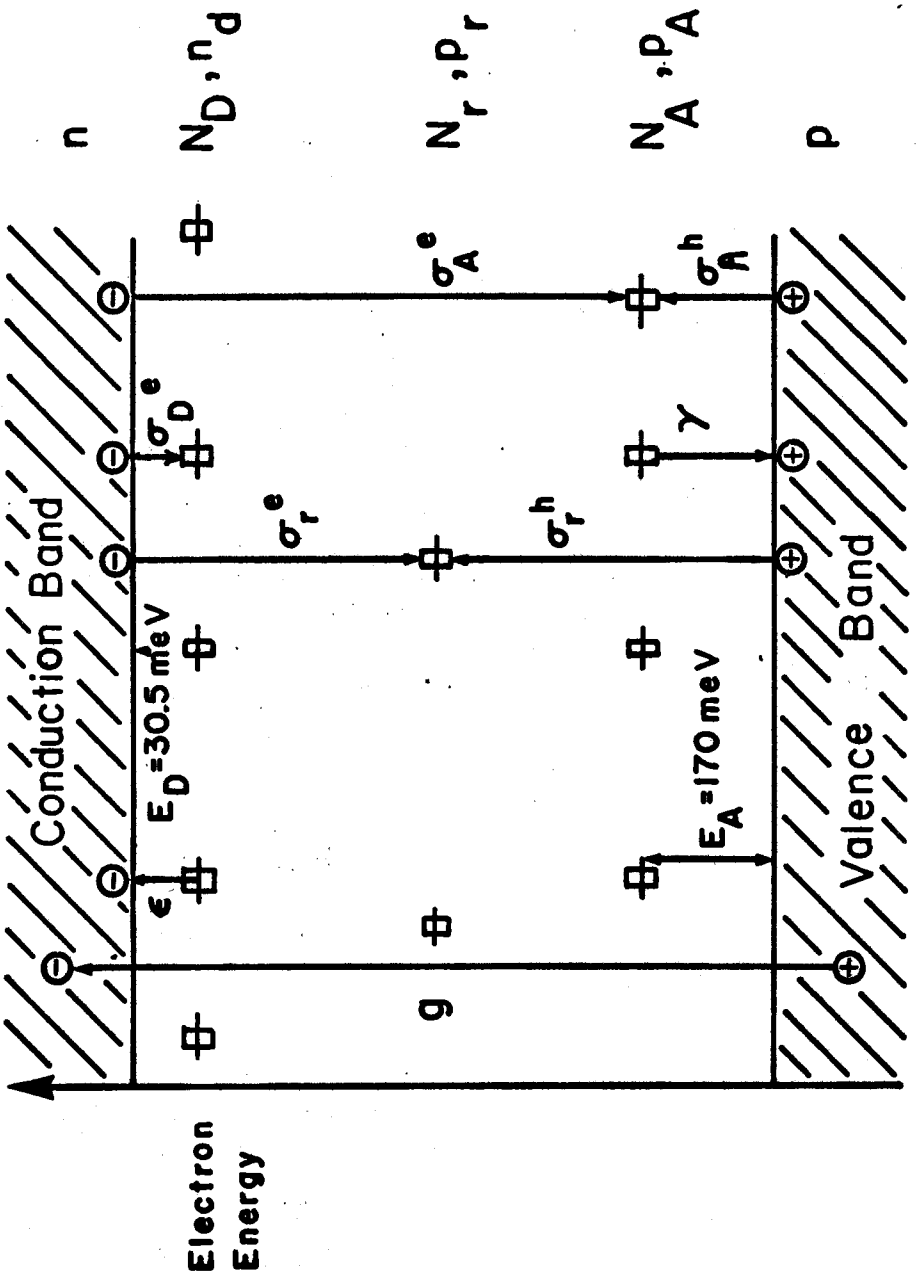

Fig. 19: Energy Band Model.

The steady-state excess free electron and hole concentrations are determined by the continuity equations:

$$\frac{d(\Delta n)}{dt} = g - \frac{\partial j_n}{\partial x} - \frac{\Delta n}{\tau_n} = 0, \tag{6-1}$$

and

$$\frac{d(\Delta p)}{dt} = g - \frac{\partial j_p}{\partial x} - \frac{\Delta p}{\tau_p} + \gamma p_A = 0, \tag{6-2}$$

where j_n and j_p are the electron and hole current densities. The hole lifetime is very short in CdS (Spear and Mort, 1963); thus, assuming that the holes will be captured first, the electron and hole recombination lifetimes are

$$\tau_n = [\sigma_A{}^e v_e p_A + \sigma_r{}^e v_e p_r]^{-1}, \tag{6-3}$$

and

$$\tau_p = [\sigma_A{}^h v_h (N_A - p_A) + \sigma_r{}^h v_h (N_r - p_r)]^{-1}, \tag{6-4}$$

where v_e and v_h are the thermal velocities of the electron and hole. Eqs. (1) and (2) cannot be solved in general.

When the gradient of the current density is zero, one obtains

$$\Delta n = g\tau_n, \tag{6-5}$$

and

$$\Delta p = (g+\gamma p_A)\tau_p, \tag{6-6}$$

where

$$g = \alpha I_o \exp(-\alpha x), \tag{6-7}$$

and

$$\gamma = \sigma_A{}^h v_h N_v \exp(-E_A/kT). \tag{6-8}$$

Here, I_o is the absorbed photon flux, α is the optical absorption coefficient, and N_v is the effective density of states in the valence band.

When current flow is important, Eqs. (1) and (2) can be solved (Appendix A) under the assumption that the ratio of electron-to-hole concentration, ρ, is independent of position. If, in addition, the ambipolar diffusion length, L_a, is large compared with the absorption length, $1/\alpha$, the free carrier concentrations are

$$\Delta n = \frac{I_o \tau_n}{L_a} \frac{1 + s_n^*/\alpha D_n}{1 + s_n^* L_a/D_n} \exp(-x/L_a), \tag{6-9}$$

and

$$\Delta p = \Delta n/\rho, \tag{6-10}$$

where s_n^* is the effective surface recombination velocity of electrons.

Two experimental observables are the photoconductivity of the photo-excited region and the photoluminescence. The transverse photoconductivity is proportional to the change in conductance,

$$\Delta G = (w/\ell)\int_o^\infty \Delta\sigma dx,$$

$$= (ew\mu_n/\ell)\int_o^\infty \Delta n(x)dx \tag{6-11}$$

where e is the electronic charge, w is the width of the electrodes, ℓ is the electrode separation, and μ_n is the electron mobility.

The photoluminescence due to the recombination of free electrons with holes trapped at acceptors is

$$L_{fb} = A\sigma_A{}^e v_e \int_o^\infty p_A n dx, \tag{6-12}$$

where A is the illuminated area. Diffusion of carriers in the y-z plane and reabsorption of the emitted radiation are neglected.

The steady-state occupations of the centers N_A and N_r are obtained from the rate equations

$$dp_A/dt = 0 = \sigma_A{}^h v_h (N_A - p_A)p - \sigma_A{}^e v_e p_A n - \gamma p_A, \tag{6-13}$$

and

$$dp_r/dt = 0 = \sigma_r{}^h v_h (N_r - p_r)p - \sigma_r{}^e v_e p_r n, \tag{6-14}$$

as

$$p_A = N_A/\left(1 + \frac{Bn}{p} + \frac{N_v \exp - E_A/kT}{p}\right), \tag{6-15}$$

and

$$p_r = N_r/\left(1 + C\frac{n}{p}\right), \tag{6-16}$$

where

$$B = \sigma_A{}^e v_e/\sigma_A{}^h v_h \quad \text{and} \quad C = \sigma_r{}^e v_e/\sigma_r{}^h v_h. \tag{6-17,18}$$

These quantities will be used in Eq. (12) to obtain formulae for the luminescence efficiency which can be compared with experimental data.

To calculate quantities which can be compared with experimental data it is necessary to compute averages for carrier concentrations and lifetimes. These averages will be taken over one absorption length $(1/\alpha)$ in the case where the current gradients are negligible, and over one ambipolar diffusion length (L_a) in

the case where L_a is large compared to $1/\alpha$. This covers about two-thirds of the free carriers generated and assumes that the remaining one-third deeper in the crystal behave similarly. In insulating crystals, it is also an excellent assumption to assume that the thermal equilibrium density of free electrons (n_o) is small compared to the photo-excited density (Δn).

In the case where the current gradients may be neglected, Eqs. (5), (7) and (11) now yield for the photoconductance efficiency

$$\eta_{pc} \equiv \Delta G/I_o = (ew\mu_n/\ell)\langle\tau_n\rangle \tag{6-19}$$

$$\text{where} \quad \langle\tau_n\rangle \equiv \int_o^{1/\alpha} \alpha\exp(-\alpha x)(\sigma_A{}^e v_e p_A + \sigma_r{}^e v_e p_r)^{-1} dx. \tag{6-20}$$

The luminescence efficiency (photons emitted per photon absorbed) is, by Eqs. (5), (7) and (12),

$$\eta_{fb} \equiv L_{fb}/AI_o = \sigma_A{}^e v_e \langle p_A \tau_n\rangle \tag{6-21}$$

$$\text{where} \quad \langle p_A\tau_n\rangle \equiv \int_o^{1/\alpha} \alpha\exp(-\alpha x) p_A(\sigma_A{}^e v_e p_A + \sigma_r{}^e v_e p_r)^{-1} dx. \tag{6-22}$$

In the case where current flow is important, and Eq. (9) applies, one obtains from Eq. (11)

$$\eta_{pc} = (ew\mu_n/\ell)\langle\tau_n\rangle \frac{1 + s_n^*/\alpha D_n}{1 + s_n^* L_a/D_n}, \tag{6-23}$$

$$\text{where} \quad \langle\tau_n\rangle \equiv \int_o^{L_a} \exp(-x/L_a) L_a^{-1} (\sigma_A{}^e v_e p_A + \sigma_r{}^e v_e p_r)^{-1} dx. \tag{6-24}$$

The luminescence efficiency is, by Eqs. (9) and (12),

$$\eta_{fb} = \sigma_A{}^e v_e \langle p_A \tau_n \rangle \frac{1 + s_n^*/\alpha D_n}{1 + s_n^*/L_a/D_n}, \tag{6-25}$$

where $\langle p_A \tau_n \rangle \equiv \int_o^{L_a} \exp(-x/L_a)(p_A/L_a)(\sigma_A{}^e v_e p_A + \sigma_r{}^e v_e p_r)^{-1} dx.$ (6-26)

It will be verified later that, under most conditions, the interpretation of the data is consistent with the assumption that the ambipolar diffusion length (L_a) is small compared to the optical absorption length ($1/\alpha$), and that for the most efficient crystal (A), which is analyzed in detail, one may also neglect the non-radiative surface recombination. Since experimentally it is found that p_A and τ_n vary slowly compared to $\exp(-\alpha x)$, the average of their product is approximately equal to the product of their averages. Defining convenient new constants, the luminescence efficiency (Eq. 21) may then be written in the form

$$\eta_{fb} = (B\eta_o/\tau_{po})(\langle p_A \rangle / N_A)\langle \tau_n \rangle, \tag{6-27}$$

where $$\tau_{po} = (\sigma_A{}^h v_h N_A + \sigma_r{}^h v_h N_r)^{-1}, \tag{6-28}$$

and $$\eta_o = (1 + \sigma_r{}^h N_r/\sigma_A{}^h N_A)^{-1}, \tag{6-29}$$

are the hole lifetime and luminescence efficiency at low excitation intensity and low temperature. In terms of the transition rate

$$1/\langle \tau_r \rangle = \{C(1-\eta_o)/\tau_{po}\}(\langle p_r \rangle / N_r), \tag{6-30}$$

involving the centers N_r, the luminescence efficiency is

$$\eta_{fb} = 1 - \langle \tau_n \rangle / \langle \tau_r \rangle. \tag{6-31}$$

Substituting for $\langle \tau_n \rangle$ and $\langle \tau_r \rangle$ from Eqs. (27) and (30), Eq. (31) may be written as,

$$1/\eta_{fb} = 1 + \frac{C(1-\eta_o)}{B\eta_o} \frac{N_A/\langle p_A \rangle}{N_r/\langle p_r \rangle} , \qquad (6\text{-}32)$$

or alternatively, using Eqs (15) and (16), one finds

$$1/\eta_{fb} = 1 + \frac{C(1-\eta_o)}{B\eta_o} \frac{1 + B\frac{\langle n \rangle}{\langle p \rangle} + \frac{N_V \exp -E_A/kT}{\langle p \rangle}}{1 + C\frac{\langle n \rangle}{\langle p \rangle}} \qquad (6\text{-}33)$$

These various forms for the luminescence efficiency will be useful in analyzing the data.

2. Data .

The data reported in this chapter are representative of measurements made on several "high-purity" cadmium sulfide crystals. Two of the crystals (A and B) are high resistivity, ($\rho_A > 10^5$ohm-cm and $\rho_B > 10^3$ohm-cm) platlets grown by the method of Frerich (1947). Crystal D is a low resistivity ($\rho_D \sim 10$ ohm-cm) crystal cut from a large single crystal obtained from the Clevite Corporation.

Fig. (20) shows the luminescence efficiency as a function of excitation intensity for the free electron-to-bound hole recombination for crystal A between 64 and 98°K. The average electron lifetime as a function of excitation intensity (Fig. 21) is derived assuming that there is negligible diffusion of the optically generated carriers. The fraction of occupied acceptors as

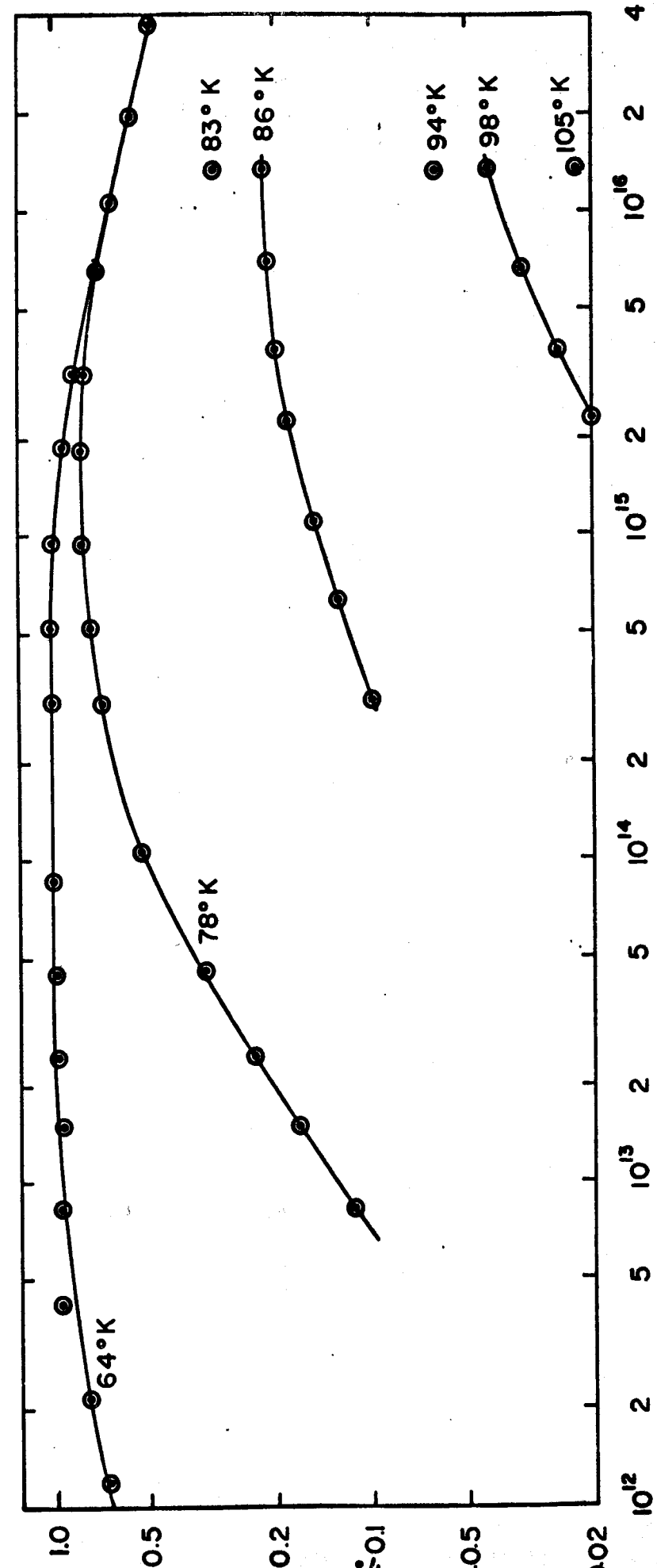

FIG. 20: LUMINESCENCE EFFICIENCY AS A FUNCTION OF EXCITATION INTENSITY

FIG. 21: AVERAGE ELECTRON LIFETIME AS A FUNCTION OF EXCITATION INTENSITY

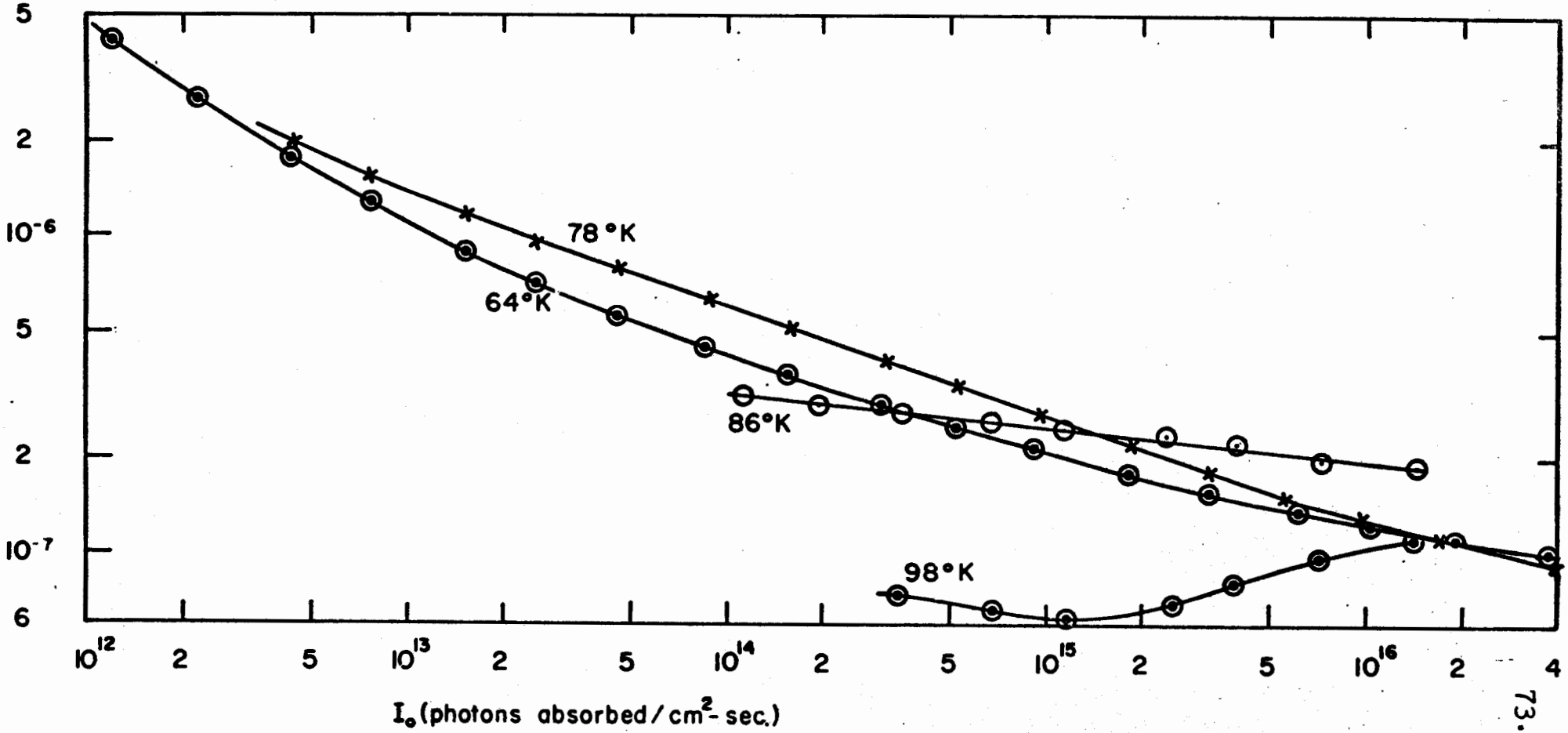

a function of excitation intensity for crystal A, (Fig. 22), was obtained from the ratio of the photoluminescence to the average electron lifetime (Fig. 20, 21). In Fig. (23), the transition rate for electrons through N_r as a function of excitation intensity was derived from the data in Fig. (20) and (21). Fig. (24) shows the free-to-bound emission efficiency as a function of excitation intensity for an insulating, a semi-insulating, and a conducting crystal at 64 and 78°K.

3. Calculation of Parameters

The data in Figs. 20 to 23 will be analyzed below to obtain values for the parameters in the theory. Their physical significance is discussed later.

(a) At low temperatures ($N_v \exp(-E_A/kT) \ll Bn$) and high excitation intensity ($Bn/p \ll 1$), from Eqs. (15) and (27),

$$\tau_{po}/B = (\eta_o/\eta_{fb})\langle\tau_n\rangle. \qquad (6\text{-}34)$$

Figs. (20) and (21) show that the luminescence efficiency is indeed proportional to the electron lifetime at high excitation intensity at 64 and 78°K. At $I_o = 2.0 \times 10^{16}/cm^2\text{-sec}$, one has $\langle\tau_n\rangle = 1.13 \times 10^{-7}$ sec and $\eta_{fb}/\eta_o = 0.59$, and thus $\tau_{po}/B = 1.90 \times 10^{-7}$ sec.

(b) A lower bound for B can be obtained from the 64°K data. At an excitation intensity of $2.0 \times 10^{13}/cm^2\text{-sec}$, the fractional occupation of N_A is 0.25 and thermal quenching is negligible since $\eta_{fb}/\eta_o \geq 0.99$. Thus, from Eq. (15), with $N_v \exp(-E_A/kT) = 9.8 \times 10^4/cm^3$ and $\langle\tau_n\rangle = 7.8 \times 10^{-7}$ sec

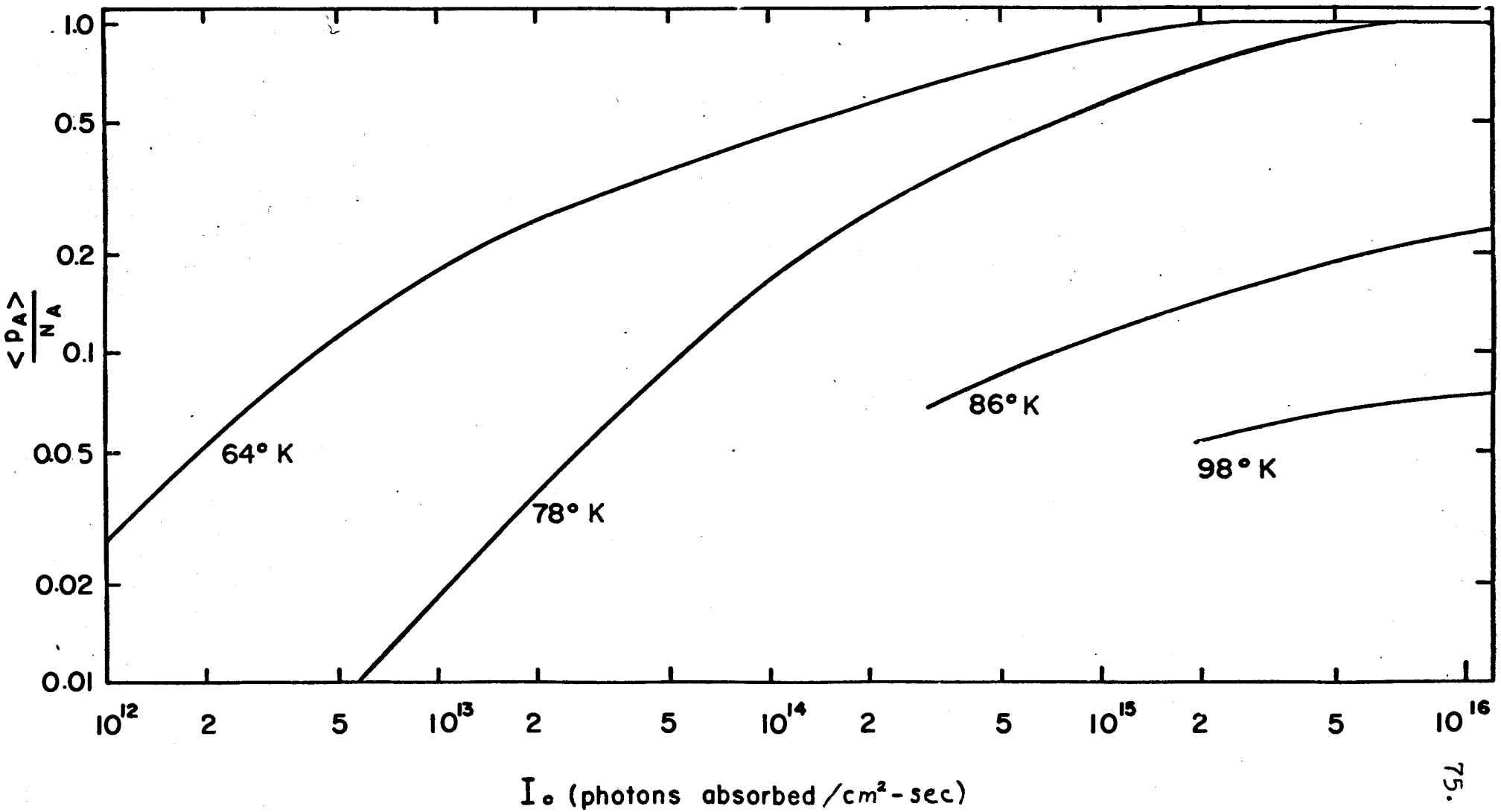

FIG. 22: FRACTION OF OCCUPIED ACCEPTORS AS A FUNCTION OF EXCITATION INTENSITY

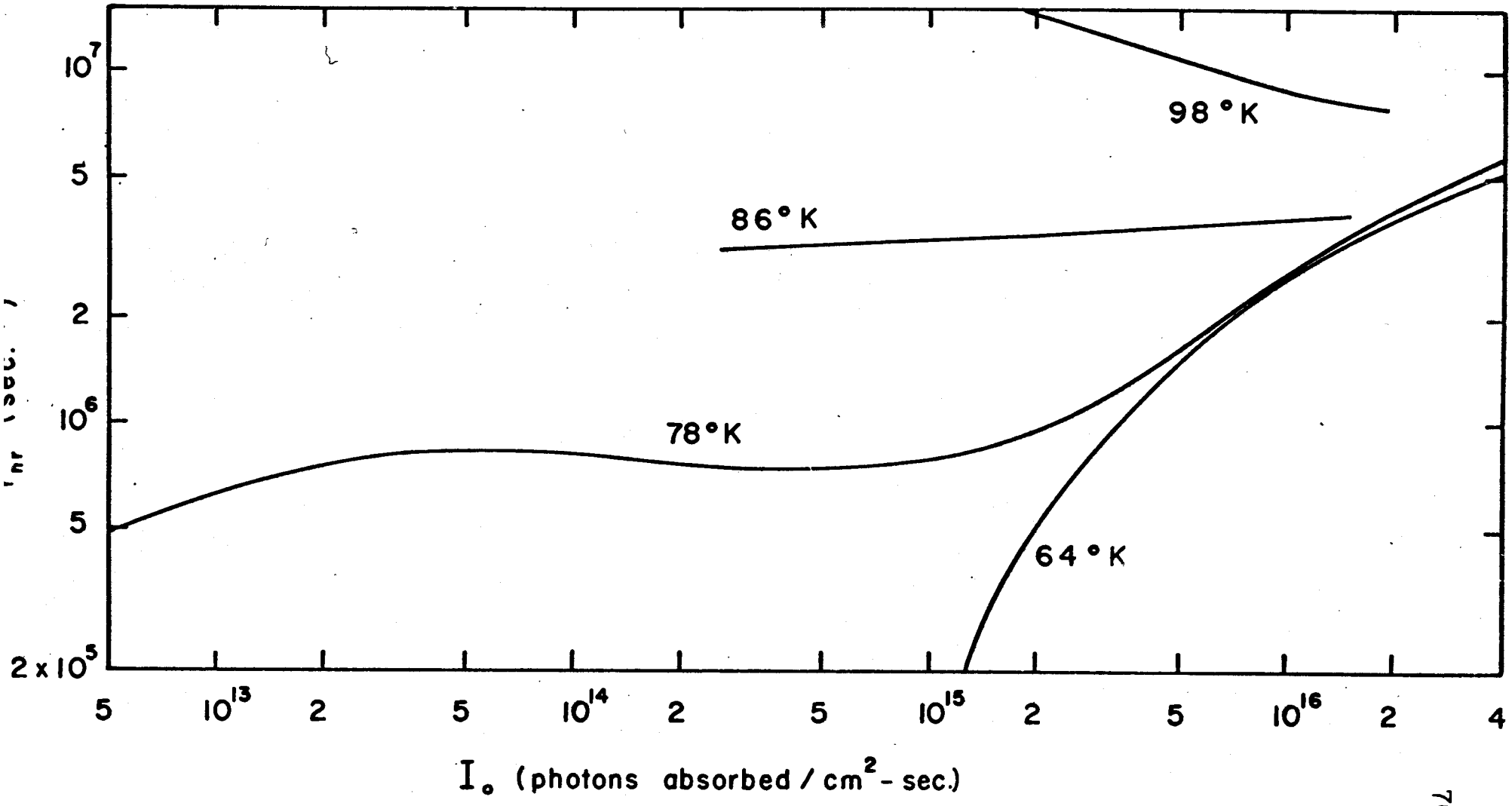

FIG. 23: NON-RADIATIVE TRANSITION RATE FOR ELECTRONS AS A FUNCTION OF EXCITATION INTENSITY

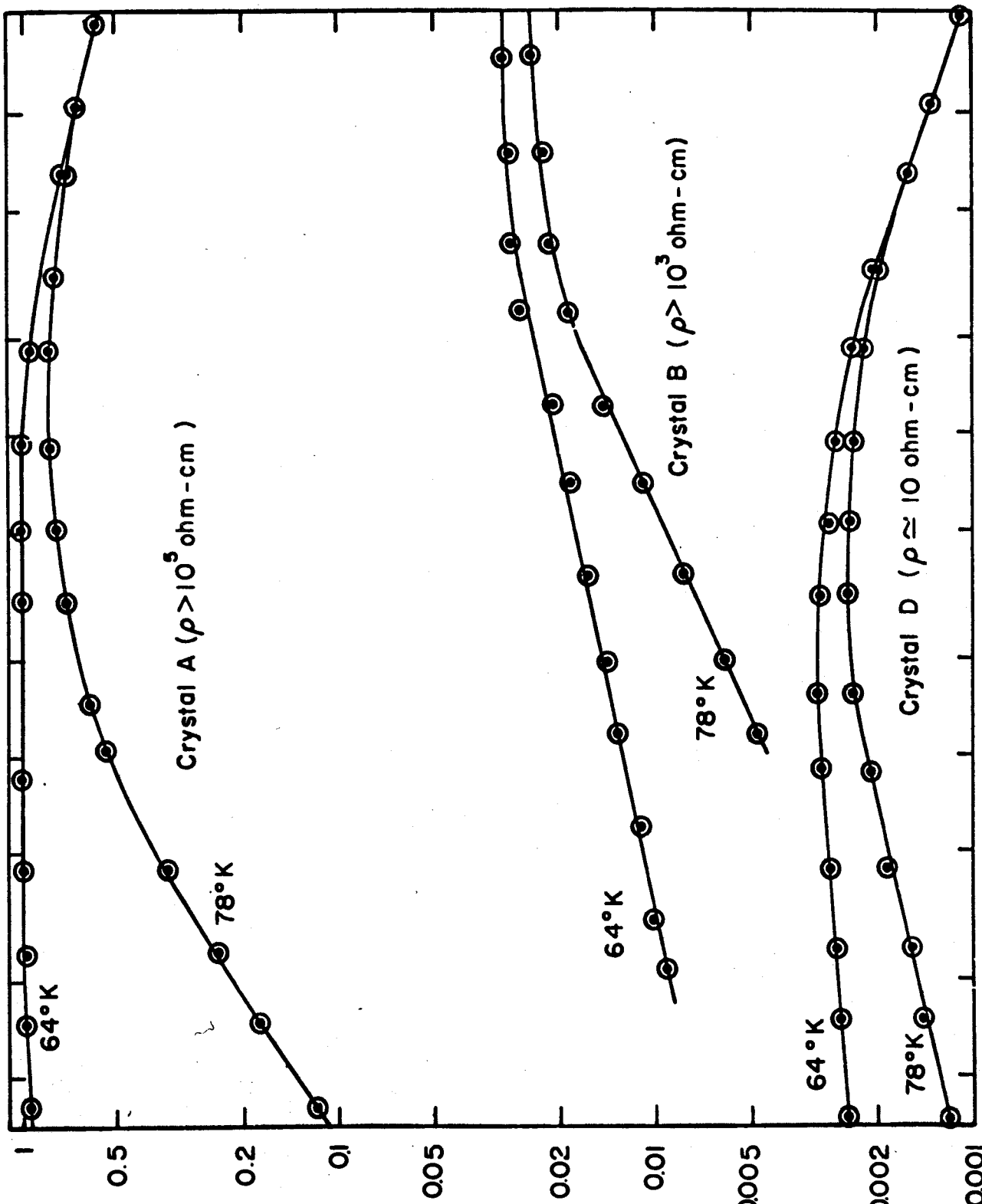

FIG. 24: LUMINESCENCE EFFICIENCY AS A FUNCTION OF EXCITATION INTENSITY FOR CRYSTALS OF VARIOUS RESISTIVITIES

$$B > (N_v \exp -E_A/kT)/n = 0.63 \times 10^{-7}. \qquad (6\text{-}35)$$

At an excitation intensity of 6.0×10^{15} photons/cm^2-sec, the luminescence efficiency is lower at 78 than at 64°K. Therefore, thermal quenching is important, and thus with $N_v \exp(-E_A/kT) = 3.3 \times 10^7/cm^3$ and $\langle \tau_n \rangle = 1.5 \times 10^{-7}$ sec,

$$B < (N_v \exp -E_A/kT)/n = 3.7 \times 10^{-7}. \qquad (6\text{-}36)$$

(c) At low temperatures, Eqs. (15) and (16) yield

$$(N_A/p_A) - 1 = (B/C)\left\{(N_r/p_r) - 1\right\}. \qquad (6\text{-}37)$$

At high excitation intensity, nearly all acceptors (N_A) are occupied (Fig. 21), but the N_r centers are not completely occupied with holes (Fig. 22). Hence, it follows that B is small compared to C.

(d) At low temperatures (64°K), and low excitation intensity ($Cn/p \gg 1$), Eq. (33) reduces to

$$\eta_o/\eta_{fb} = \eta_o + (1-\eta_o)(1 + p/Bn). \qquad (6\text{-}38)$$

For $I_o = 2.0 \times 10^{13}/cm^2$-sec, one has $\eta_{fb}/\eta_o \geq 0.99$ and $\langle p_A \rangle / N_A = 0.25$. From Eq. (15), $p/Bn = 0.33$ and hence $\eta_o \geq 0.97$.

(e) At 78°K, and low excitation intensity, thermal quenching of the luminescence is dominant ($N_v \exp -E_A/kT \gg p$), and hence Eq. (33) simplifies to

$$\eta_{fb}/\eta_o = \left\{B/(1-\eta_o)\right\}\left\{\alpha I_o \langle \tau_n \rangle / N_v \exp - E_A/kT\right\}. \qquad (6\text{-}39)$$

At $I_o = 6.0 \times 10^{12}/cm^2$-sec, one has $N_v \exp -E_A/kT = 3.3 \times 10^7/cm^3$, $\langle \tau_n \rangle = 1.72 \times 10^{-6}$sec, and $\eta_{fb}/\eta_o = 0.15$. Using the range of B determined in (b), one obtains

$$0.92 < \eta_o < 0.99. \qquad (6\text{-}40)$$

4. Dependence of the Luminescence Efficiency on Excitation Intensity and Temperature

The most extensive study was done on crystal A since it has a very low dark conductivity and is thus expected to follow the theory in detail. At 64^oK, the thermal ionization rate of trapped holes (γ) is negligible for excitation intensities above 2.0×10^{13} photons/cm^2-sec, and thus the luminescence efficiency is constant and equal to η_o, as shown in Fig. (20). For excitation intensities above $10^{15}/cm^2$-sec, all the N_A acceptors are occupied with holes, as shown in Fig. (22). Any further electron-hole pairs created by the light must then decay at the N_r sites, and hence the green free-to-bound efficiency goes down with further increase in excitation intensity. At 78^oK, thermal ionization of holes from the acceptors (N_A) is effective in lowering the luminescence efficiency at all except the highest excitation intensities, where the thermal ionization rate of holes becomes negligible compared to the radiative recombination rate with free electrons. At higher temperatures, the thermal ionization rate of the bound holes is always large compared to the rate of recombination with free electrons. Thus the acceptor (N_A) acts as a trap, rather than a recombination center, and the holes

are free long enough to be captured by the N_r recombination centers, or the surface.

At very low excitation intensity, an additional complication may arise, which could explain the decrease in the luminescence efficiency at 64°K: Holes may be swept to the surface by an electric field due to chemisorbed oxygen ions. At higher excitation intensity, the increased free carrier density screens out this field and the effect disappears (Ch. IV). However, the thermal quenching alone may account for the decrease in efficiency.

5. The Physical Significance of B, C, τ_{po} and η_o

The average values obtained for crystal A from the data at 64 and 78°K are $\eta_o = 0.98$, $B = 2 \times 10^{-7}$, $\tau_{po} = 4 \times 10^{-14}$ sec and $C >> B$. These parameters yield capture cross-sections which are discussed below.

Using the definitions of the parameters, and the above values one finds, from Eqs. (15), (28), and (29),

$$\sigma_A^e = B\eta_o/\tau_{po}v_eN_A = 5 \times 10^6/v_eN_A. \qquad (6\text{-}41)$$

The room temperature dark conductivity of crystal A is 3.7×10^{-7}/ohm-cm. With $\mu_n = 250$ cm^2/V-sec (Spear and Mort, 1963), one finds $n = 9.2 \times 10^9$/cm^3. Since a typical donor concentration for these crystals is 10^{16}/cm^3 (Colbow, 1966), and since at these temperatures most of the donors would be ionized, the crystals are well compensated and $N_A \simeq 10^{16}$/cm^3. With $m_e^* = 0.20m_o$ (Spear and Mort, 1963), the electron velocity is

$$v_e = (3kT/m_e^*)^{\frac{1}{2}} = 1.2 \times 10^7 \text{cm/sec} \qquad (6\text{-}42)$$

at 64°K, and thus,

$$\sigma_A{}^e = 4 \times 10^{-17} \text{cm}^2, \qquad (6\text{-}43)$$

which is a reasonable value for the capture cross-section of a neutral center (Lax, 1959). Using this value in the definition of B (Eq. 15), the capture cross-section for a hole by the ionized acceptor is

$$\sigma_A{}^h = \sigma_A{}^e v_e/Bv_h = 4 \times 10^{-10} \text{cm}^2. \qquad (6\text{-}44)$$

This value for $\sigma_A{}^h$ is in reasonable agreement with what one obtains by assuming that for a coulomb attractive capturing center all free carriers with kinetic energy less than the coulomb energy will be captured. Thus,

$$e^2/\kappa r = 3kT/2 \qquad (6\text{-}45)$$

determines the radius around the acceptor inside which carriers will be captured, and the cross-section is, for T = 64°K and κ = 10.3 (Berlincourt et al, 1963),

$$\sigma_A{}^h = \pi r^2 = 4\pi e^4/9\kappa^2 k^2 T^2 = 1 \times 10^{-11} \text{cm}^2. \qquad (6\text{-}46)$$

The parameter C involves the capture cross-section of the recombination center, N_r, and is contained in the recombination rate, $\langle r_r \rangle$. At low temperature, this rate only becomes important when the free-to-bound transition rate, becomes saturated (Figs. 22, 23). An estimate for C can be obtained by noting that $\langle r_r \rangle$

seems to saturate ($\langle p_r \rangle = N_r$) at about 10^5/sec at 64 and 78°K. Thus, from Eq. (30),

$$C = \tau_{po}\langle r_r \rangle/(1-\eta_o\rangle = 2 \times 10^{-5}, \qquad (6\text{-}47)$$

which satisfies the criterion C >> B established earlier. Since holes are captured first, and $C = \sigma_r{}^e v_e/\sigma_r{}^h v_h$ is small compared to unity, this center must be an acceptor; in which case $\sigma_r{}^h$ is coulomb attractive and $\sigma_r{}^e$ is capture by a neutral center. Some further comments on this center are made in Section 7 of this Chapter.

At low excitation intensity and low temperature, the internal luminescence efficiency, $\eta_o = 0.98$, is high due to the rapid capture of the free holes by the acceptor involved in the green luminescence (N_A), compared to the slower capture by the other recombination center (N_r). The external quantum efficiency may be much lower due to non-radiative surface recombination in conjunction with reabsorption near the surface of the internally reflected luminescence.

The hole recombination lifetime (τ_{po}) is much shorter than the values of 10^{-6} to 10^{-9} sec reported elsewhere (Spear and Mort, 1963). The reason for this apparent discrepancy is that τ_{po} is the free hole recombination lifetimes at low temperature and low excitation intensity where all the acceptors are active as fast capturing centers. Longer lifetimes are observed (Spear and Mort, 1963) at higher temperature, where the acceptors (N_A) act only as trapping centers and hence the holes do not recombine until they are captured at the deeper and "slower" recombination

sites (N_r). When the hole lifetime becomes longer, the diffusion of free carriers out of the photo-excited region will likely become an important process.

6. Dependence of the Luminescence Efficiency on Resistivity

The theory for the luminescence efficiency was based on the assumption that the thermal free electron density (n_o) is small compared to the photo-excited free electron density (Δn). The luminescence efficiencies of crystals B and D, in which the thermal electron densities are not small, are shown, along with the data for crystal A, in Fig. (24). The more conducting crystals have a lower luminescence efficiency. All three of the crystals are high-purity and are thought to contain about $10^{16}/cm^3$ donors due to foreign impurities (Colbow, 1966); however, the conducting crystals are less well compensated by cadmium vacancy acceptors (Handelman and Thomas, 1965) and hence have fewer sites at which the green free-to-bound luminescence can originate. Thus the relative importance of other recombination sites increases.

One also observes that the slope of the luminescence efficiency at 78°K and low excitation intensity decreases for low resistivity crystals. Thermal quenching of the luminescence is dominant and Eq. (33) simplifies to

$$\eta_{fb}/\eta_o = \left\{B/(1-\eta_o)\right\}\left\{\langle n\rangle/N_v \exp(-E_A/kT)\right\} \qquad (6\text{-}48)$$

where

$$\langle n\rangle = n_o + \langle \Delta n\rangle. \qquad (6\text{-}49)$$

For the high-conductivity crystal (D), for which Δn is small compared to n_o, the luminescence efficiency should only have a weak dependence on excitation intensity, as observed (Fig. 24). For the insulating crystal (A), the luminescence efficiency is proportional to $I_o \tau_n$ as predicted, and the intermediate case, crystal B, exhibits an intermediate slope.

7. Red Luminescence and Non-Radiative Recombination

At high excitation intensities, the green emission transitions become saturated (Figs. 20, 22) and further increase of excitation intensity results in a greater fraction of the recombination taking place at the other recombination center (N_r), as shown in Fig. (23). The center N_r represents an effective recombination center density and is probably composed of states at several energy levels in the forbidden band gap.

It is shown in Section 5, that N_r is an acceptor-type center. Assuming that the neutral capture cross-section, σ_r^e, is approximately the same as the neutral capture cross-section of the cadmium vacancy acceptor, σ_A^e, we find (using the data in Section 5) that $\sigma_r^h \simeq 1 \times 10^{-12} cm^2$. This coulomb attractive capture cross-section is smaller by a factor of 25 than σ_A^h, the capture cross-section for the cadmium vacancy acceptor involved in the green light emission. One may expect the cross-sections to be proportional to the square of the Bohr radius, or inversely proportional to the square of the ionization energy of the center. Since $E_A = 0.17$ eV, one predicts that the center N_r is about 0.85 eV above the valence band. One might then expect

a free electron-to-bound hole emission band at 7000 Å and emission at 1.46 microns due to hole capture by the N_r center. We found an emission band at 7000 Å for this crystal (Fig. 25); however, its intensity and dependence on excitation level (Fig. 26) indicate that this emission accounts for only a fraction of the recombination through N_r. An emission band at 7200 Å which was quenched by 1.41 micron radiation has previously been observed and attributed to copper impurities (Broser and Broser-Warminsky, 1957). This red emission band is still present at higher temperatures where the green emission has been quenched due to thermal ionization of the cadmium vacancy acceptors.

Thus, although some of the recombination through the centers, N_r, may be radiative, most of it is non-radiative. Non-radiative recombination processes are not well understood, although they probably occur at clusters of impurities and defects. From the values of η_o, N_A and the capture cross-sections, the effective recombination center density is $N_r = 8 \times 10^{16}/cm^3$.

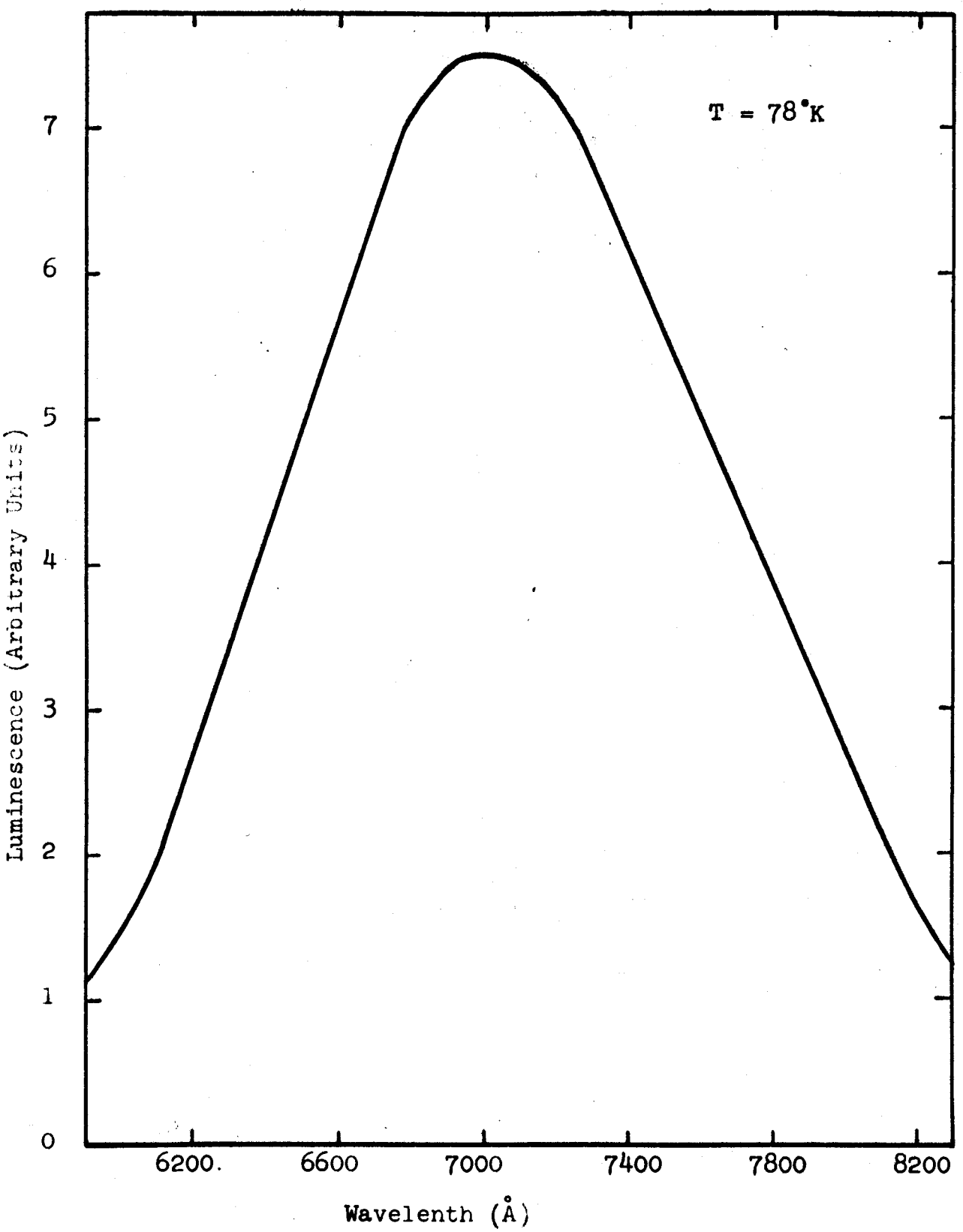

FIG. 25: RED LUMINESCENCE SPECTRUM

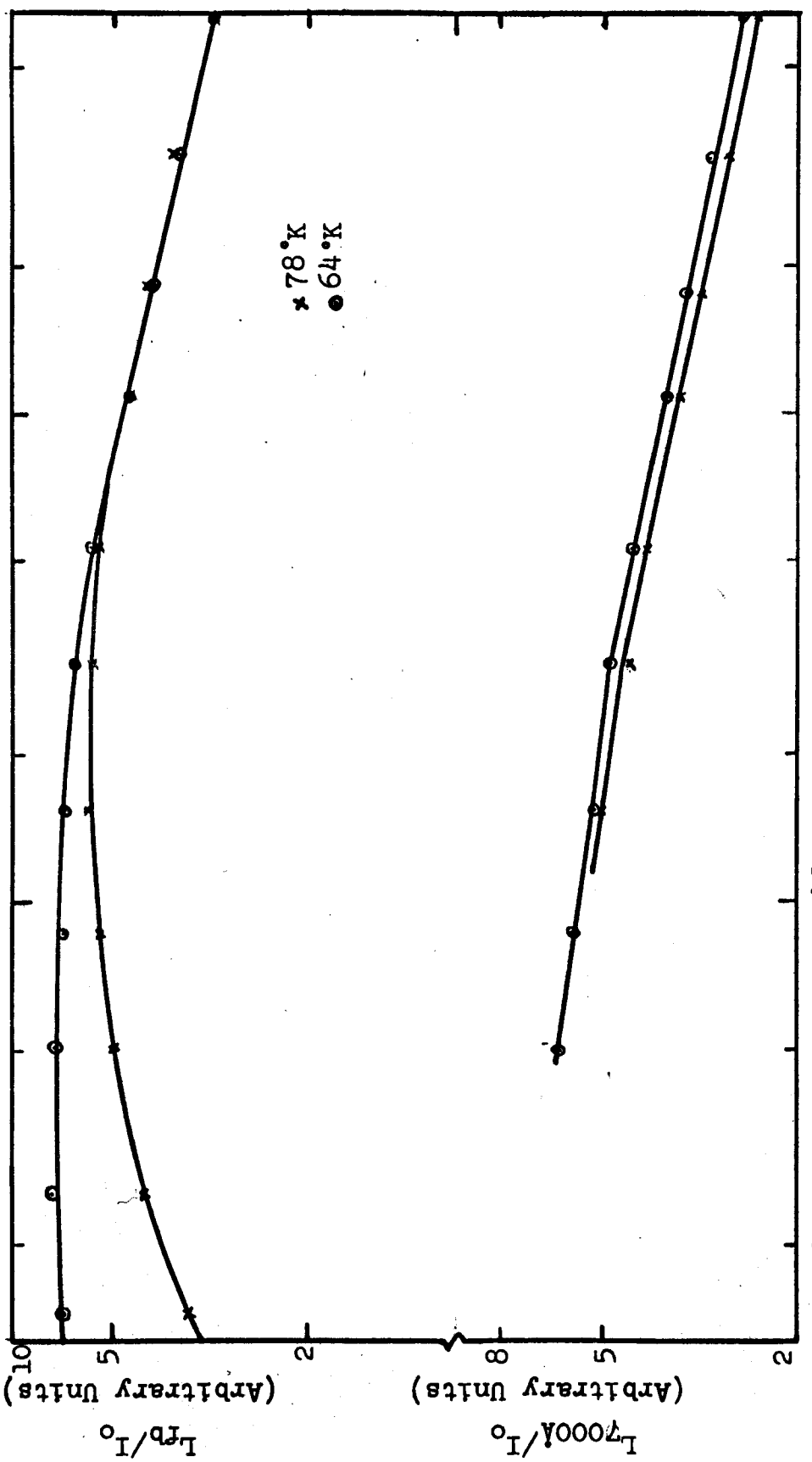

FIG. 26: COMPARISON OF THE LUMINESCENCE EFFICIENCIES OF THE RED (7000Å) AND THE GREEN (f-b) EMISSION BANDS

CHAPTER VII

SUMMARY AND CONCLUSIONS

The recombination kinetics in photo-excited cadmium sulfide crystals have been studied experimentally and the data analyzed in detail in terms of a simple, but realistic, energy band model. This model consists of the foreign impurity donors and cadmium vacancy acceptors previously established as being involved in the luminescence (Colbow, 1966). In addition, an effective recombination center density (consisting of deep acceptor-like recombination centers) and non-radiative surface recombination centers are required to account for the data on luminescence efficiency and surface effects on luminescence. The results of the thesis are divided into four chapters and these are summarized below.

Chapter III deals with the controversy, existing in the literature at the onset of the study, regarding the origin of the high energy green emission band. It had been shown (Collins, 1959; Pedrotti and Reynolds, 1960; Colbow, 1966) on the basis of extensive experimental data, that this band could only be understood on the basis of a free-to-bound transition; however, Maeda (1965) and Condas and Yee (1966), on the basis of their data, concluded that it was of the bound-to-bound type. The interpretation of the recombination kinetics of this band is dependent on its origin and hence it was necessary to resolve these conflicting views. Further analysis and experiments showed that Maeda interpreted his data incorrectly while Condas and Yee's

data was also not in conflict with the free-to-bound interpretation. This work is summarized in two papers (Colbow and Nyberg, 1967a; 1967b).

The second topic (Ch. IV) was the effect of non-radiative surface recombination on the luminescence efficiency. The conclusions were that extrinsic surface states, due to chemisorbed oxygen ions, are associated with non-radiative surface recombination. This recombination is aided by the electric field set up in the charge depletion layer next to the chemisorbed oxygen ions. The polarity of the field is such as to draw holes to the surface and the luminescence efficiency can be enhanced by applying an external electric field of opposite polarity or by photo-desorbing the oxygen ions. An external field of the same polarity as the depletion layer field quenches the luminescence. The experiments on luminescence efficiency as a function of excitation wavelength showed the effects of non-radiative surface recombination in that the shortest wavelength excitation (where the carriers are produced closest to the surface) yielded the lowest efficiency. The experiments on surface effects were difficult to do reproducibly and this is believed to be, at least in part, because the surface state density changes slowly during the experiment. This work is summarized in a paper by Nyberg and Colbow (1967a). Further experiments in this area should include the investigation of evaporating transparent insulating layers on the surface of CdS to stabilize it. It was also found (Nyberg and Colbow, 1967b) that heating CdS briefly in a nitrogen ambient produces free-to-bound and bound-to-bound

transitions associated with nitrogen acceptors 130 meV above the valence band.

The third topic (Ch. V) was the recombination kinetics of free and bound excitons, and the bound electron-to-bound hole luminescence. Higher excitation intensity favors higher exciton emission efficiency for all crystals and for the range of excitation intensity available. This is expected in-so-far as the formation of excitons depends on the product of the free carrier densities. The bound-to-bound emission efficiency is high and varies only slowly with excitation intensity since the donors and acceptors involved in these transitions have very high capture cross-sections for the free carriers. High excitation intensity favors recombination at donor-acceptor pairs of close separation. It would be of interest to investigate the recombination kinetics of the exciton, bound-to-bound and free-to-bound emissions to the much higher excitation intensities available with a pulsed electron beam source. At very high excitation intensity, if one obtains a significant density of free holes, one would expect to see the free hole-to-bound electron transition. Room temperature green luminescence should also be observable at very high excitation intensity.

The last topic studied (Ch. VI), and the most important from the standpoint of quantitative information obtained, was the study of the recombination kinetics of the free electron-to-bound hole transition. Using the model discussed earlier, the data was analyzed to obtain the electron and hole lifetimes, the luminescence efficiency, and the electron and hole capture

cross-sections of the cadmium vacancy acceptor and the other deep recombination center. The hole lifetime is shown to be very short and this (along with the interpretation of the surface effects) rules out diffusion into the interior of the crystal as a significant process at low temperatures. The internal luminescence efficiency is unexpectedly high and this is due to the high capture cross-section of the cadmium vacancy acceptors for free holes. Some of the recombination at the deeper recombination center is shown to be radiative; however, most of it is non-radiative. This work is summarized in a paper by Colbow and Nyberg (1967b). Future work in this area should include the effects on the luminescence efficiency of different concentrations of the donors, cadmium vacancy acceptors, and the effective recombination center density. A better understanding of non-radiative processes in wide-band-gap materials is also required.

APPENDIX A

Free carriers are generated in an insulator by highly absorbed optical radiation at a rate

$$g(x) = \alpha I_0 e^{-\alpha x}, \tag{A1}$$

where I_0 is the absorbed photon flux and $\alpha(\lambda)$ is the absorption coefficient. Under continuous excitation, the spatial distribution of the free carriers is governed by the continuity equations:

$$g(x) - \partial j_n/\partial x - n/\tau_n = 0, \tag{A2}$$

$$g(x) - \partial j_p/\partial x - p/\tau_p = 0; \tag{A3}$$

the equations of current flow,

$$j_n = -n\mu_n E - D_n(\partial n/\partial x), \tag{A4}$$

$$j_p = p\mu_p E - D_p(\partial p/\partial x); \tag{A5}$$

conservation of current,

$$j_n + j_p = 0; \tag{A6}$$

and Poisson's equation,

$$(\epsilon/e)(\partial E/\partial x) = (p-n) - (N_A-p_A) - (N_r-p_r) + (N_D-n_D), \tag{A7}$$

where it is assumed that the nonradiative recombination centers are acceptor-like states.

Substituting (A4) and (A5) into (A2) and (A3) gives

$$g - \frac{n}{\tau_n} + D_n\frac{d^2n}{dx^2} + \mu_n\frac{d}{dx}(En) = 0 \tag{A8}$$

and

$$g - \frac{p}{\tau_p} + D_p \frac{d^2p}{dx^2} - \mu_p \frac{d}{dx}(Ep) = 0, \tag{A9}$$

where

$$1/\tau_n = \sigma_A {}^e v_e p_A + \sigma_r {}^e v_e p_r \tag{A10}$$

and

$$\frac{1}{\tau_p} = \frac{n}{p} \frac{1}{\tau_n} . \tag{A11}$$

In general, it is not possible to solve (A8) and (A9), because τ_n and τ_p are functions of n and p. However, they can be solved under the assumption that

$$n(x)/p(x) = \rho, \tag{A12}$$

where ρ is a constant (Mark 1965a).

Substituting (A11) in (A9), multiplying (A8) by μ_p and (A9) by $\rho\mu_n$, and adding the resulting equations gives

$$g(x) - \frac{n(x)}{\tau_n} + D_a \frac{d^2n}{dx^2} = 0, \tag{A13}$$

where

$$D_a = 2D_n/(1 + b\rho) \tag{A14}$$

and

$$b = \mu_n/\mu_p = D_n/D_p. \tag{A15}$$

Following deVore (1956), substitute (A1) in (A13) to obtain

$$\frac{d^2n}{dx^2} = \frac{n}{L_a^2} - \frac{\alpha I_0}{D_a} e^{-\alpha x} , \tag{A16}$$

the general solution of which is

$$n(x) = Be^{-x/L_a} + Ce^{x/L_a} + \frac{\alpha I_0}{D_a} \frac{1}{(1/L_a^2) - \alpha^2} e^{-\alpha x}, \tag{A17}$$

where

$$L_a = (D_a \tau_n)^{\frac{1}{2}} . \tag{A18}$$

The sample is thick compared to the absorption length ($1/\alpha$) and the ambipolar diffussion length (L_a) and thus the constant C is zero. Representing the electron recombination current at the surface by the surface recombination velocity of electrons (s_n), the boundary condition is:

$$j_n(0) = -n(0)s_n. \tag{A19}$$

Using Equation (A19), the spatial distribution of electrons is

$$n(x) = \frac{\alpha I_0 \tau_n}{1 - (\alpha L_a)^2} \left\{ e^{-\alpha x} - \frac{s_n - \mu_n E(0) + \alpha D_n}{s_n - \mu_n E(0) + D_n/L_a} e^{-x/L_a} \right\} \tag{A20}$$

It is convenient to introduce the concept of an effective surface recombination velocity for electrons (s_n^*), given by

$$s_n^* = s_n - \mu_n E(0). \tag{A21}$$

Equation (A20) may now be written

$$n(x) = \frac{\alpha I_0 \tau_n}{1 - (\alpha L_a)^2} \left\{ e^{-\alpha x} - \frac{s_n^* + \alpha D_n}{s_n^* + D_n/L_a} e^{-x/L_a} \right\} . \qquad (A22)$$

BIBLIOGRAPHY

Auth, J., 1961. J. Phys. Chem. Solids 18, 261.

Bancie-Grillot, M., Gross, E. F., Grillot, E. and Razbirin, B. S., 1959. Optika i Spectroskopiya 5, 461.

Berlincourt, D., Jaffe, H. and Shiozawa, L. R., 1963. Phys. Rev. 129, 1009.

Blakemore, J., 1962. Semiconductor Statistics, (Pergamon Press) p. 135.

Bleil, C. E. and Broser, I, 1964. Proc. 7th Intern.-Conf. Phys. Semiconductors, Paris 1964, p. 897.

Broser, F. and Broser-Warminsky, R., 1957. Zeitschrift fur Elektrochemie, 71, 209.

Bube, R. H., 1953. J. Chem. Phys. 21, 1409.
1956. Phys. Rev. 101, 1668.

Colbow, K., 1965. Phys. Rev. 139, A274.
1966. Phys. Rev. 141, 742.

Colbow, K. and Nyberg, D. W., 1967a. Phys. Letters, 25A, 250.
1967b. J. Phys. Chem. Solids, to be published.

Condas, G. A. and Yee, J. H., 1966. Appl. Phys. Letters, 9, 188.

Collins, R. J., 1959. J. Appl. Phys., 30, 1135.

DeVore, H. B., 1956. Phys. Rev., 102, 86.

Eckart, F. and Asch, M., 1961. Z. Physik 164, 529.

Frerich, R., 1947. Phys. Rev., 72, 594.

Furlong, F. R., 1954. Phys. Rev., 95, 1086.

Furlong, L. R. and Ravilious, C. F., 1955. Phys. Rev., 98, 954.

Gross, E. F., Razbirin, B. S. and Permogorov, S. F., 1965. Soviet Phys.-Solid State, 7, 444.

Gross, E. F., Nedzvetsky, D. S., 1964. Proc. 7th Intern. Conf. Phys. Semiconductors, Paris, 1964; Vol. 4, Symp. on Radiative Recombination, Dunod, Paris 1965, p. 81.

Hall. J. F., 1956. J. Opt. Soc. Am., 46, 1013.

Halsted, R. E. and Segall, B., 1963. Phys. Rev. Letters, 10, 392.

Handelman, E. T. and Thomas, D. G., 1965. J. Phys. Chem. Solids, 26, 1261.

Hopfield, J. J., 1959. J. Phys. Chem. Solids, 10, 110.

Klick, C. C., 1951. J. Opt. Soc. Am., 41, 816.

Kroger, F. A., 1940. Physica, 7, 1.

Kroger, F. A. and Meyer, H. J. G., 1954. Physica, 20, 1149.

Lambe, J. J., Klick, C. C. and Dexter, D. L., 1956. Phys. Rev., 103, 1715.

Lax, M., 1959. J. Phys. Chem. Solids, 8, 66.

Levine, J. D. and Mark, P., 1966. Phys. Rev., 144, 751.

Liebson, S. H. 1955. J. Chem. Phys., 23, 1732.

Maeda, K., 1965. J. Phys. Chem. Solids, 26, 1419.

Many, A. and Katzir, A., 1967. Surface Science, 6, 279.

Mark, P., 1964, J. Phys. Chem. Solids, 25, 911; 1965a, Phys. Rev., 137, A203; 1965b, J. Phys. Chem. Solids, 26, 1767.

Markelois, E. P., Lavine, M. C., Mariano, A. N. and Gatos, H. C., 1962. J. Appl. Phys. 33, 690.

Nyberg, D. W. and Colbow, K., 1967a. Can. J. Phys., 45, 2833. 1967b. Can. J. Phys., 45, 3333.

Park, Y. S. and Reynolds, D. C., 1963. Phys. Rev. 132, 2450.

Pedrotti, L. S. and Reynolds, D. C., 1960. Phys. Rev., 119, 1897.

Razbirin, B. S., 1964. Soviet Physics-Solid State, 6, 256.

Reed, C. E. and Scott, C. G., 1964. Brit. J. Appl. Phys., 15, 1045.

Reynolds, D. C. and Litton, C. W., 1963. Phys. Rev., 132, 1023.

Reynolds, D. C., Litton, C. W. and Collins, T. C., 1965. Phys. stat. sol., 9, 645; 12, 3.

Ryvkin, S. M. and Khansevarov, R. I., 1958. Soviet Physics-Technical Physics, 3, 862.

Seitz, F., 1940. The Modern Theory of Solids, (McGraw-Hill, 1940), p. 409 ff., p. 447 ff.

Seraphin, B., 1953. Ann. Physik Leipzig, 13, 198.

Smith, R. W., 1955. Phys. Rev., 97, 1525.

Spear, W. E. and Bradberry, R., 1965. Phys. stat. sol. 8, 649.

Spear, W. E. and Mort, J, 1963. Proc. Phys. Soc., 81, 130.

Tamm, I., 1932. Physik Z. Sowjetunion, 1, 733.

Thomas, D. G. and Hopfield, J. J., 1959. Phys. Rev., 116, 573.
1961. Phys. Rev. Letters, 7, 316.
1962. Phys. Rev., 128, 2135.

Thomas, D. G., Gershenzon, M. and Trumbore, F. A., 1964. Phys. Rev., 133A, A269.

Thomas, D. G., Hopfield, J. J., and Colbow, K., 1964. Proc. 7th Intern. Conf. Physics Semiconductors, Paris 1964; Vol. 4, Symp. on Radiative Recombination (Dunod, Paris 1965), p. 67.

Williams, R., 1962. J. Phys. Chem. Solids, 23, 1057.

Winogradoff, N. N., 1961. J. Appl. Phys., 32, 506.

Woodbury, H. H., 1964. Phys. Rev., 134, A492.